SANDIA REPORT

SAND2013-9385
Unlimited Release
Printed October 2015

The Initial Atmospheric Transport (IAT) Code: Description and Validation.

Charles W. Morrow, SNL
Timothy J. Bartel, SNL

Prepared by
Sandia National Laboratories
Albuquerque, New Mexico 87185 and Livermore, California 94550

Sandia National Laboratories is a multi-program laboratory managed and operated by Sandia Corporation, a wholly owned subsidiary of Lockheed Martin Corporation, for the U.S. Department of Energy's National Nuclear Security Administration under contract DE-AC04-94AL85000.

Issued by Sandia National Laboratories, operated for the United States Department of Energy by Sandia Corporation.

Available to DOE and DOE contractors from
U.S. Department of Energy
Office of Scientific and Technical Information
P.O. Box 62
Oak Ridge, TN 37831

Telephone:	(865) 576-8401
Facsimile:	(865) 576-5728
E-Mail:	reports@adonis.osti.gov
Online ordering:	http://www.osti.gov/bridge

Available to the public from
U.S. Department of Commerce
National Technical Information Service
5285 Port Royal Rd.
Springfield, VA 22161

Telephone:	(800) 553-6847
Facsimile:	(703) 605-6900
E-Mail:	orders@ntis.fedworld.gov
Online order:	http://www.ntis.gov/search/sitesearch.aspx

SAND2013-9385
Unlimited Release
Printed October 2015

The Initial Atmospheric Transport (IAT) Code: Description and Validation.

Charles W. Morrow and Timothy J. Bartel

Sandia National Laboratories, P.O. Box 5800, Albuquerque, NM 87185, USA

ABSTRACT

The Initial Atmospheric Transport (IAT) computer code was developed at Sandia National Laboratories as part of their nuclear launch accident consequences analysis suite of computer codes. The purpose of IAT is to predict the initial puff/plume rise resulting from either a solid rocket propellant or liquid rocket fuel fire. The code generates initial conditions for subsequent atmospheric transport calculations.

The Initial Atmospheric Transfer (IAT) code has been compared to two data sets which are appropriate to the design space of space launch accident analyses. The primary model uncertainties are the entrainment coefficients for the extended Taylor model [1, 2]. The Titan 34D accident (1986) was used to calibrate these entrainment settings for a prototypic liquid propellant accident while the recent Johns Hopkins University Applied Physics Laboratory (JHU/APL, or simply APL) large propellant block tests (2012) were used to calibrate the entrainment settings for prototypic solid propellant accidents. North American Meteorology (NAM)formatted weather data profiles are used by IAT to determine the local buoyancy force balance. The IAT comparisons for the APL solid propellant tests illustrate the sensitivity of the plume elevation to the weather profiles; that is, the weather profile is a dominant factor in determining the plume elevation. The IAT code performed remarkably well and is considered validated for neutral weather conditions.

Acknowledgements

The authors of this paper wish to acknowledge the extensive contributions from authors at ASCA Inc., NASA's Kennedy Space Center (KSC), and the Jet Propulsion Laboratory (JPL) for the Multi-Mission Launch Vehicle Databooks (Databooks). This report relies heavily upon those works. The authors also wish to thank Ryan Bechtel, Yale Chang, Stephen Giannino, and Scott Hopkins for their many detailed reviews of the DSAR, and Laura Connolly for sustained technical writing support. Finally, the authors wish to thank Ryan Bechtel of DOE's Office of Space and Defense Power Systems for his steadfast support and encouragement in this effort.

Table of Contents

Table of Figures

Table of Tables

1 Introduction

The Initial Atmospheric Transport (IAT) computer code was developed at Sandia National Laboratories (SNL) as part of their suite of nuclear launch accident consequences analysis computer codes. The purpose of IAT is to predict the initial puff/plume rise resulting from either a solid rocket propellant or liquid rocket fuel fire. This information provides the initial conditions for subsequent atmospheric transport calculations.

This report describes the code in Chapter 2 and then documents Sandia's validation of it in Chapters 3 for liquid propellant fires and Chapter 4 for solid propellant fires.

This report compares IAT simulations to measured puff or plume rise data from two events:

- Titan 34D explosion during launch in April 1986 (liquid propellant fire)
- Recent solid rocket propellant tests conducted for nuclear launch safety purposes on the behalf of DOE (solid propellant fire)

After minor adjustment to one input parameter for the liquid propellant fire only, the IAT code performed remarkably well and is considered validated for neutral weather conditions.

The Titan 34D rocket accident occurred in April 1986 when a Titan rocket fueled by a liquid hydrazine mixture exploded shortly after launch. The resulting cloud of burned liquid fuel was tracked by two video cameras. Shortly after the accident, investigators analyzed these videos using photogrammetry to estimate puff rise with time. The incident very closely resembles the type of accident that could occur during a launch involving nuclear fuels and liquid fuel fires. As such the puff trajectory data provides a good test of IAT's ability to predict the consequences of a liquid-fueled fire.

The Johns Hopkins University Applied Physics Laboratory (JHU/APL, or simply APL) conducted tests in June of 2012 in support of the SNL nuclear launch accident analysis team using a typical solid propellant and conditions representative of predicted solid propellant fires. As with the Titan 34D incident, the plume resulting from the tests was captured by two video cameras. This data allowed Sandia to estimate plume trajectory using photogrammetry. The tests very closely simulate the type of burns expected during a near-ground solid propellant burn. Therefore, they provide another relevant case for the validation of the IAT code.

2 Initial Atmospheric Transport Code Description

The Initial Atmospheric Transport, IAT, computer program was written to predict the initial puff/plume rise resulting from either a solid rocket propellant or liquid rocket fuel fire. The code generates initial conditions for subsequent atmospheric transport calculations. The code is written to be compiled using a FORTRAN 90 compiler.

2.1 Assumptions

IAT assumes that the plume/puff is modeled as a well-mixed sphere (control volume) which rises to some height, *z*. The plume is assumed to be an ideal gas. The well mixed control volume assumption implies a uniform gas temperature, species concentration, and pressure. The pressure of the plume is assumed to be in equilibrium with the atmospheric pressure at a height, *h*. A model for the control volume 'skin temperature' is used for thermal radiation heat transfer. Atmospheric wind can advect this control volume. These assumptions are graphically illustrated in Figure 1 for both a no-wind and transverse wind environments.

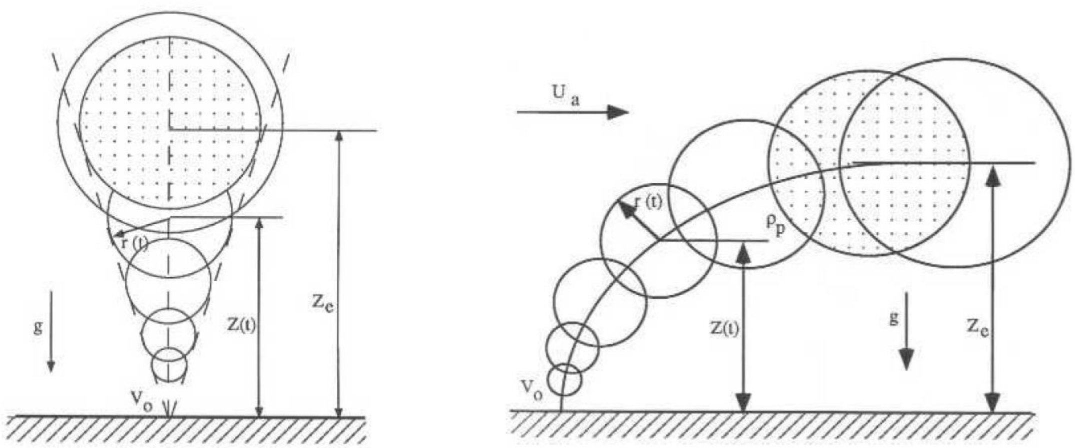

Figure 1: Illustration of IAT Assumptions [1]

2.2 Conservation Equations

The processes which affect the plume rise mechanics are shown in Figure 2. Note that all chemical reactions are assumed to have completed prior to the design space which IAT considers; that is, at IAT time 0.0, the combustion processes are assumed to have finished.

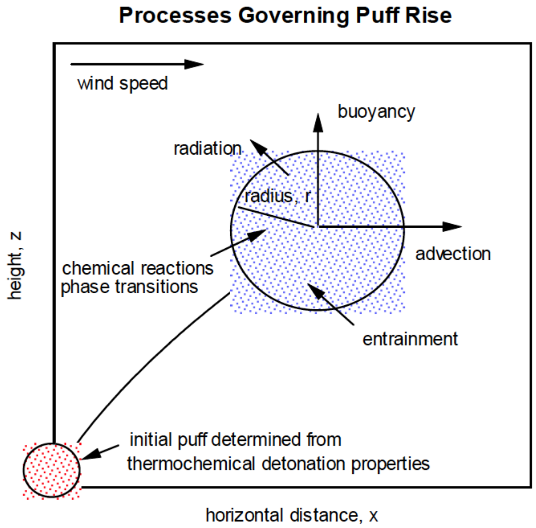

Figure 2: Processes Governing Puff Rise

The processes outlined in Figure 2 can be expressed as the conservation of mass, momentum, and energy. The respective rates of change form a system of ODEs:

Rate of change of puff mass (due to entrainment):

$$\frac{dm}{dt} = pd^2 a\left|V_e\right| r_\infty = pd^2 r_\infty\left[a_1\left|V_z - V_{z_\infty}\right| + a_2\left|\bar{V}_l - \bar{V}_{l_\infty}\right| + a_3\frac{\sqrt{2\cdot TKE}}{3}\right] \tag{1}$$

Rate of change of momentum (with virtual mass considerations):

$$\frac{dP_z}{dt} = \left(\rho_\infty - \rho_{fb}\right) g\left(\tfrac{4}{3}\pi r^3\right) - \left(\tfrac{1}{2}C_D\rho_\infty\left(V_z\right)^2\right)\left(4\pi r^2\right) + \dot{m}_{entrainment}V_{z_\infty}, \tag{2}$$

$$\frac{dP_x}{dt} = \left(\tfrac{1}{2}C_D r_{¥}\left(V_x\right)^2\right)\left(4pr^2\right) + \dot{m}_{entrainment}V_{x_{¥}} \tag{3}$$

Rate of change of enthalpy (energy):

$$\begin{aligned}\frac{dh}{dt} &= h_\infty\left[\pi d^2\alpha\left|V_r\right|\rho_\infty\right] - \left(\tfrac{4}{3}\pi r^3\rho_{fb}\right) gV_z \\ &-\left(\tfrac{1}{2}C_D\rho_\infty V_r^2\right)\left(4\pi r^2\right)V_z \\ &-\varepsilon\sigma(\pi d^2)((\gamma T_{puff})^4 - T_{amb}^4) + h_{cond}\cdot\dot{m}_{cond}\end{aligned} \tag{4}$$

Rate of change in displacement (for each direction x, y, z):

$$\frac{dz}{dt} = V_z \tag{5}$$

The IAT code uses a standard Runge-Kutta-Fehlburg order 4(5) solver, or RKF45, to advance the solution in time.

Table 1 contains a list of variables used in the five equations above.

Table 1: Summary of Variables

P	Description	Units
C_D	Drag coefficient	--
r or d	Puff radius or diameter	*m*
h	Specific enthalpy including heat of formation	*J/kg*
m	Puff mass	*kg*
m_{vm}	Puff mass and virtual mass	*Kg*
p	Puff momentum	*N·s*
TKE	Atmospheric turbulent kinetic energy	*J/kg*
V	Velocity	*m/s*
V_{puff}	Puff volume	m^3
x,y	Transverse coordinates	*m*
z	Puff centerline elevation	*m*
α	Entrainment coefficient	--
γ	Skin temperature factor (default = 0.2)	--
ε	Emissivity (default = 0.2)	--
ρ	Density	Kg/m^3
σ	Stefan-Boltzmann constant = 5.670376E-08	$W/m^2/K^4$
Subscripts		
e	Entrainment	
∞	Freestream atmospheric conditions	
1,2,3	Entrainment model indices	
z	Elevation	
l	Lateral *(x, y)*	
fb	Fireball or plume	
puff	Conditions in puff	
cond	Condensate	

It should be noted that the mass (m_{vm}) in the momentum equation is the mass of the puff and the virtual mass; that is, the effective mass due to the motion of an accelerating body through a fluid. Therefore the mass in the z-momentum balance is defined as:

$$m_{vm} = (m_{puff} + \tfrac{1}{2}\rho_{air}V_{puff}) \tag{6}$$

where $r_{air}V_{puff}$ is the mass of air displaced by the puff.

2.3 Entrainment Model

Entrainment is a complex fluid dynamic mixing phenomenon that occurs in the mixing layer between two fluids with a relative velocity. IAT uses a simple empirical formulation based on the classical G. I. Taylor entrainment model [1, 2] and extended to explicitly include turbulent effects [4] to capture this stochastic process.

Given a Cartesian $\hat{i}, \hat{j}, \hat{k}$ coordinate system where the *i* unit vector points due north, the *j* unit vector points east and the *k* unit vector points upward (elevation), the ambient velocity, **V**, can be decomposed into the following steady ($\bar{u}, \bar{v}, \bar{w}$) and time varying ($u', v', w'$) quantities:

$$\mathbf{V} = (\bar{u} + u')\hat{i} + (\bar{v} + v')\hat{j} + (\bar{w} + w')\hat{k} \tag{7}$$

Similarly for the puff,

$$\mathbf{V}_p = \left(\bar{u}_p + u'_p\right)i + \left(\bar{v}_p + v'_p\right)j + \left(\bar{w}_p + w'_p\right)k \tag{8}$$

The IAT code estimates entrainment as a mass flux driven by vertical shear between the ambient air and the plume as it rises, horizontal shear between the ambient wind and the plume and turbulent fluctuations. The total entrainment mass rate is a sum of these three effects where the unknowns are the three entrainment velocities.

$$\begin{aligned} &\dot{m}_{entrainment} = A_{surface}\rho_{ambient}V_{entrainment} \\ &where \\ &A_{surface} = 4\pi R_{puff}^{2} \\ &V_{entrainment} = \left(\alpha_1 V_1 + \alpha_2 V_2 + \alpha_3 V_3\right) \end{aligned} \tag{9}$$

The entrainment velocities are defined as:

$$V_e = \sqrt{\left(\bar{w} - \bar{w}_p\right)^2} \tag{10}$$

$$V_e = \sqrt{\left(\bar{u} - \bar{u}_p\right)^2 + \left(\bar{v} - \bar{v}_p\right)^2} \quad (11)$$

$$V_e = \frac{1}{3}\sqrt{2TKE} \quad (12)$$

The Turbulent Kinetic Energy, TKE, is normally provided by the NAM weather data file, or calculated based on a correlation with temperature gradient (see section 2.8). The α_1, α_2, and α_3 are empirical constants to be determined from experimental data (discussed later in this report). Typical literature values range from 0.1 to 0.65. The entrainment velocity is limited to be greater than a user supplied lower bound (default is 0.2 m/s)

2.4 Equation of State

While the energy equation (4) is for total internal energy, the gas temperature is required to determine fluid enthalpy. Therefore, an equation of state model is used to obtain the real gas temperature given mixture component properties and species mole fractions. The gas temperature of the puff gas mixture is determined by posing the problem as finding the root of: $0 = H^{n+1} - \tilde{H}(T^{n+1})$, where ($H^{n+1}$) is the known enthalpy at the updated time step and (T^{n+1}) is the puff temperature. $\tilde{H}$ is obtained from functional fits of the specific heat for the various puff gas species (excerpted from the JANAAF tables) [5]. This function is highly non-linear and therefore a Newton-Raphson root finder was used to iteratively solve for the updated temperature.

2.5 Water Vapor Condensation Model

Since the plume cools as it rises in the atmosphere, IAT must allow for the water vapor in the plume to condense into liquid drops. First, the local saturated water vapor pressure, $E_w{}^*$, is determined by the relationship

$$E_w^* = 6.1121 \cdot \left(1.0007 + 3.46E-06P\right) e^{\frac{17.502 \cdot T}{240.97+T}} \quad (13)$$

where puff pressure, P, is in hPa, puff temperature, T, is in °C and E_w^* is also in hPa [6]. The relative humidity in IAT is defined as the ratio of the partial pressure of water vapor (in hPa) to E_w^* and is limited to 1.0; that is, no supersaturated states. This limit provides an upper bound on the local water vapor pressure and thus the local water vapor mole fraction. The heat of condensation for the condensed water is added to the energy (enthalpy) of the puff. This energy increases the temperature of the puff and therefore its buoyancy as well as increasing its final rise height.

There are two possible options to describe the handling of condensed water in IAT. In option 1 (variable *icondense*), the condensate drops settle out of the rising puff/plume. Therefore the mass of the puff/plume is reduced to account for the transfer of mass from vapor to liquid phase. In option 2 (*icondense* = 2), the condensate drops are kept in the puff during its rise; that is a *cloud* is formed. This is the default option.

Figure 3 compares the rise heights for a case where the relative humidity would be greater than 1.0 during the rise with the condensation model off and also for the condensation option 2. One can see that the relative humidity would achieve a non-physical value of greater than 1.4 without the model while it is limited to 1.0 with the model. Also the plume rises approximately 10% higher with the condensate model on. Again, this is the default configuration.

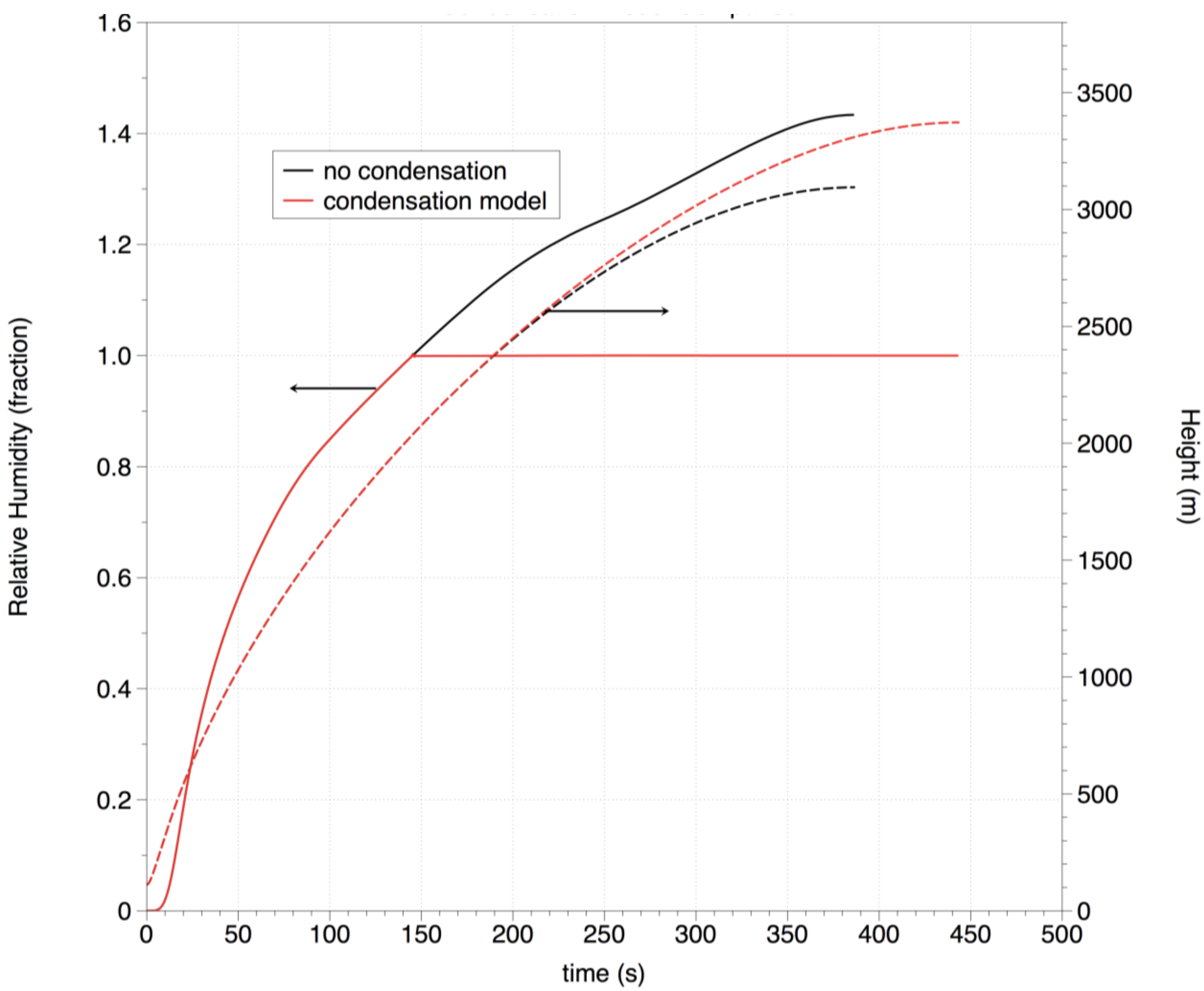

Figure 3: IAT Condensation Model Comparison

2.6 Initial Conditions

The plume is assumed to be an ideal gas; that is the following Ideal Gas Law can be used to establish a consistent set of initial conditions.

$$P \cdot V = m\left(\frac{\bar{R}}{Mwt}\right)T \tag{14}$$

where

$$\begin{aligned}
&P = \text{pressure } \left(\text{N/m}^2\right)\\
&V = \text{volume} = {}^{1}\!/_{6}\,\pi \text{d}^3 \left(m^3\right)\\
&m = \text{mass } \left(g\right)\\
&Mwt = \text{molecular weight } \left(\frac{g}{mole}\right)\\
&\bar{R} = \text{universal gas constant} \left(8.314\ {}^{\text{J}}\!/_{\text{K} \cdot \text{mole}}\right)\\
&T = \text{temperature } \left(K\right)
\end{aligned} \tag{15}$$

The plume pressure is assumed to be in pressure equilibrium with the environment; this value will be provided by the weather profiles (section 0). The molecular weight will be provided in the following tables from the mole fractions of the combustion products for the liquid propellant, solid propellant or solid explosive. The unknown variables are volume (that is initial diameter of the plume), mass and temperature and therefore models or assumptions are required to determine a consistent thermodynamic state. Strategies to determine these three variables are different for each of the propellant configurations. The EOS package in IAT allows for 14 species in addition to air to be modeled so that the products of the propellant burn can be correctly included. Three different propellant configurations are included in IAT: a liquid propellant composed of RP1 & Liquid H_2 & Hydrazine, a propellant based on ammonium perchlorate & aluminum particles, and a solid explosive based on C4. The initial species mole fractions of the combustion products (for fuel species only) for each configuration are shown in the following tables. The liquid propellant fuels are assumed to react with the on-board liquid oxygen with reaction fuel mass fractions of 0.2636, 0.15555 and 0.18898 for the RPI, liquid H_2 and hydrazine fuels respectively. Here this fraction is defined as the ratio of the mass of fuel to mass of fuel and oxidizer.

Table 2: Liquid Fuels – Products of Combustion Mole Fractions

Id	species	RP1	liquid H_2	hydrazine
0	AIR			
1	CO	0.2985	0.0000	0.0000
2	CO_2	0.1634	0.0000	0.0000
3	H	0.0535	0.0012	0.0077
4	H_2	0.0825	0.0114	0.3268
5	H_2O	0.3252	0.3030	0.6166
6	N_2	0.0000	0.7565	0.0000
7	NO	0.0000	0.0001	0.0000
8	O	0.0295	0.0004	0.0069
9	O_2	0.0474	0.0044	0.0053

The mole fractions in Table 2 sum to unity. This is not necessary as IAT always normalizes product lists as part of its analysis.

2.6.1 Liquid Propellant:

Typically the total mass of the liquid propellant (fuel and oxidizer) is known for the initial configuration. Empirical relationships have been produced to relate the initial fireball diameter to the initial mass (see for example Gayle & Bransford, [7]:

$$d_{puff} = 3.769 m_{puff}^{0.325} \tag{16}$$

In equation (16), the diameter, d_{puff}, has units of meters and the mass of the puff, m_{puff}, is specified in kilograms. However, it was found that using this relationship combined with the mole fractions in Table 2 over-predicted the gas temperature. This is because the molecular weight and the diameter correlation assume no air entrainment during the burning process; the molecular weight and volume would be larger with entrainment and the temperature lower. Therefore several input options were included in IAT to resolve this issue and are enumerated in the code input section (section 2.10).

2.6.2 Solid Propellant

The solid propellant fire initial state differs from either the liquid propellant or solid explosive cases in that liquid propellant or solid explosive fuel burns very quickly (less than a second) while the solid propellant burn times are on the order of tens to hundreds of seconds. Therefore the propellant mass is not an appropriate variable; pictures taken during the 2012 APL fire tests [8] suggest that the initial plume diameter may be a function of the propellant diameter (a plume diameter of 5 times the propellant diameter is suggested by the photographs). Two unknowns remain: temperature and mass (or density). Based on Fluent simulations of the propellant burn (bottom and side burning), a temperature of approximately 2600 K appears reasonable for the initial plume temperature. The final rise height is not sensitive to this value. Therefore the initial state of the solid propellant plume is defined for the IAT simulation.

The above discussion for input conditions for solid propellants was for a single propellant fragment; an additional model was included in IAT to treat the case of multiple propellant fragments which are located close enough that the plume exhibits a collective behavior rather than a superposition from the individual fragments. This model is based on area averaging of the bounding circle of fragments; that is, the fraction of the circle which is comprised of a plume from each fragment and the remaining fraction which is comprised of gas at local atmospheric conditions. The new single plume has an area weighted temperature and species concentration (molecular weight). This model naturally collapses to the single solid propellant fragment model.

The species mole fractions of the initial solid propellant plume are given in Table 3. Since the plume characteristic dimension is typically greater than the typical 1.5 meter burn length for an aluminum drop, this distribution assumes complete combustion of the aluminum (taken from the NASA Data Book - values from Price).

Table 3: Solid Propellant – Products of Combustion Mole Fractions

Id	Species	SRP mole fractions
0	AIR	0.325
1	CO	0.26
2	CO_2	0.015
3	H	-
4	H_2	0.30
5	H_2O	0.1
6	N_2	-
7	NO	-
8	O	-
9	O_2	-
10	OH	-
11	Al	-
12	Al_2O_3	-
13	HCl	-
14	Cl	-

Table 3 contains a complete list of the possible products allowed by IAT. In the case of solid propellant, only five are used. As before, the five components' mole fractions in this case add to 1.0. This is not necessary as IAT always normalizes product lists as part of its analysis.

2.6.3 Solid Explosive

The three variables required to specify the initial plume conditions resulting from a conventional solid explosive (such as C4, RDX) are mass, diameter and temperature. Typically the explosive mass and energy density (e.g. *MJ/kg*) are known. Correlations for the initial diameter based on the energy density are available for the following two configurations [9]:

Above ground explosion:

$$d = 2.0 \cdot 0.704 \cdot \left(\frac{E}{P} \right)^{0.333} \tag{17}$$

Ground level explosion:

$$d = 2.0 \cdot 0.856 \cdot \left(\frac{E}{P} \right)^{0.333} \tag{18}$$

In the above two equations, the parameter d represents puff diameter in meters, the parameter E denotes explosive energy in Joules and P designates ambient pressure *(Pa)*.

The temperature of the initial plume is taken to be 678K based on published literature [10]. The species mole fractions of the initial plume from a solid explosive (assume C4 explosive: RDX - $C_3H_6N_6O_6$) are given in Table 4 . One will note that now all the variables in the ideal gas relationship are specified and they will probably be thermodynamically inconsistent; that is, the problem is over defined. To resolve this, it is assumed that additional mass will be entrained during the explosion and therefore an iteration loop is performed to vary the amount of air entrainment to achieve consistency; that is, the puff mass and molecular weight are updated which also changes the puff density. Convergence is typically achieved in three iterations.

Table 4: Expected Puff Mole Fractions Resulting from a C4 Explosion [10]

Id	Species	RDX mole fractions
0	AIR	-
1	CO	0.33333
2	CO_2	-
3	H	-
4	H_2	-
5	H_2O	0.33334
6	N_2	0.33333
7	NO	-
8	O	-
9	O_2	-
10	OH	-
11	Al	-
12	Al_2O_3	-
13	HCl	-
14	Cl	-

2.7 Weather Data Formats

Four different weather data formats are supported by IAT. Three are different NAM formats and the fourth is a user defined data set. The IAT code will automatically detect which of the three NAM data sets are used. The input parameter to specify the weather file is discussed in Section 2.10.

Refer to the appendix; Section Appendix A, for descriptions of each of the four weather data file formats.

2.8 Turbulent Kinetic Energy (TKE)

One will note that profiles of the TKE are input values on the first two NAM data formats and the user defined profile; the third NAM format does not have the TKE profile. The NAM files' definition of TKE is:

$$TKE = \frac{1}{2}\left(u'^2 + v'^2 + w'^2\right) \tag{19}$$

The units of TKE are specific energy (e.g. J/kg).

As noted in the discussion of the entrainment model, section 2.3, the TKE profile is explicitly used in this model. Since this profile is associated with the atmospheric boundary layer, its effect is near the ground surface. The solid propellant plume rise is very sensitive to this profile since its initial plume size is much smaller than the liquid propellant formed plume. Consequently, IAT must address the lack of TKE data in the third NAM weather data format.

The following strategy was used to compute the missing TKE profile for this NAM data set. The TKE profile was computed using the following correlation based on the local temperature gradient ($\frac{dT}{dz}$):

$$TKE = 0.599 - 26.09\frac{dT}{dz} + 848.59\left(\frac{dT}{dz}\right)^2, \; s_{EY} = 0.124 \qquad (20)$$

The standard error of the estimate, s_{ey}, results from the regression analysis and is a measure of the goodness of fit of the data to the regression form chosen.

Figure 4 contains a plot of TKE versus temperature gradient that was used to develop this correlation.

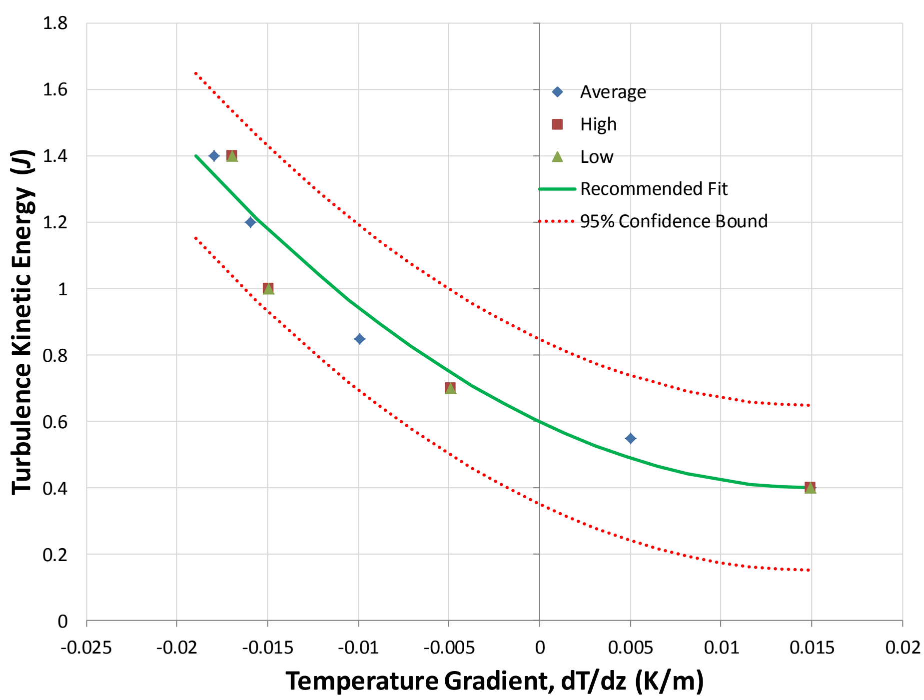

Figure 4: Plot of TKE vs. dT/dz Correlation

The temperature gradient information was extracted from Beychok [13] while the TKE data came from Wharton et al.[14] The reader will note that progressively more negative gradients result from increased insolation, resulting in more turbulent or higher TKE values.

Table 5: Stability Class vs. Temp Gradient and TKE

Class	Description	Temperature Gradient (K/m)				TKE (Joules)		
		Low	High	Average		Low	High	Average
A	Very Unstable		-0.01896	-0.01896		1.4		1.4
B	Unstable	-0.01896	-0.01695	-0.01796		1.4		1.4
C	Slightly Unstable	-0.01695	-0.01495	-0.01595		1	1.4	1.2
D	Neutral	-0.01495	-0.00492	-0.00994		0.7	1	0.85
E	Slightly Stable	-0.00492	0.01495	0.005015		0.4	0.7	0.55
F	Stable	0.01495		0.01495			0.4	0.4

The correlation was determined using the Generalized Reduced Gradient (GRG) nonlinear optimization method [15]. Criteria imposed on the method are as follows:

- Fit is assumed to be a quadratic polynomial of the form:

$$TKE = a_0 + a_1\left(\frac{dT}{dz}\right) + a_2\left(\frac{dT}{dz}\right)^2 \quad (21)$$

- Minimize the sum of the square of the residuals, $\sum_{i=1}^{n}\left(y_i - \hat{y}_i\right)^2$, where y_i is the measured TKE for a given temperature gradient and $\hat{y}_i$ is the result of the correlation for TKE at that same gradient.
- Slope of the correlation must be less than or equal to zero at dT/dz = 0.015 (extremely stable conditions)

$$\left.\frac{d\,(TKE)}{d\left(dT/dz\right)}\right)_{\frac{dT}{dz}=0.015} \leq 0 \quad (22)$$

- Value of TKE at dT/dz = -0.018 (Extremely unstable conditions) must approximate 1.4 *J*. Specifically:

$$\left|TKE_{dT/dz=-0.018} - 1.4\right| \leq 0.001 \quad (23)$$

The GRG progressively refined estimates of a_0, a_1, and a_2 while holding to the criteria listed above. The standard error of the estimate, s_{EY}, is based on the same statistic used in linear regression analysis

$$s_{EY} = \sqrt{\frac{\sum_{i=1}^{n}\left(y_i - \hat{y}_i\right)^2}{n-5}} \tag{24}$$

The denominator in equation (24) depends on the number of degrees of freedom already consumed in estimating y_i. The data were fit to a quadratic with three parameters plus an additional two constraints (equations (23) and (24)) were imposed on the solution for a total of 5 constraints. Within this envelop, the standard error of the estimate, s_{EY}, equals 0.124. For comparison, a pure linear regression analysis with only the three constraints associated with the quadratic returns a fit with s_{EY} = 0.102. However, the regression approach returns a correlation containing a local minimum within the range of temperature gradients one can expect, something that is physically not possible.

2.9 Plume Rise Termination Criterion

There are many criterions one could use to terminate the puff rise. Simply stopping the simulation when the height reaches a steady value is too simplistic when the atmospheric turbulence is included in the entrainment. That is, turbulence entrainment is essentially a dispersion mechanism and will occur without any net motion of the puff centroid. As noted in the entrainment section (2.3), a threshold is applied to the entrainment velocity since the goal of IAT it to compute the puff trajectory based on the initial buoyant force from the propellant burn/explosion. There are two stopping mechanisms in IAT. The first is to terminate the simulation if an oscillating puff has experienced four oscillations (this is a very rare event since TKE is now used as an entrainment mechanism). The second method is based on the net vertical velocity. The stopping velocity is the maximum of 1/2 of the local turbulent velocity and a user input value (default is 0.2 m/s). Again, with the use of TKE for entrainment, the termination criteria is the local turbulent velocity. As stated earlier, when the puff velocity is within the local turbulent velocity, its motion is now dominated by the turbulent entrainment induced dispersion rather than by thermal buoyant forces.

2.10 Input Description

The IAT code asks for a sequence of input parameters as a command line. The following provides the general format for the command line call:

IAT `puff_init amb_init value1 value2 value3 value4 value5 value6 value7 value8 ientrain alpha1 alpha2 alpha3 vent_min icondense zinitial`

The reader should refer to Appendix A for a detailed discussion of how the various parameters relate under different circumstances. In addition, the reader can refer to Section 3.4 (Titan 3D Explosion) and 4.2 (Solid Rocket Propellant) for examples of command line usage.

The input variable *puff_init* controls the type of burn:

1. Liquid propellant with initial diameter and initial temperature specified
2. Liquid propellant with RP1, liquid hydrogen and hydrazine masses specified in USC units
3. Liquid propellant with RP1, liquid hydrogen and hydrazine masses specified in SI units
4. Solid rocket propellant with initial diameter and initial temperature specified
5. Solid rocket propellant for multiple sources with initial diameter and initial temperature and parameter to identify multiple plume area specified
6. Above ground C4 explosive, C4 mass and energy density specified
7. Ground level C4 explosive, C4 mass and energy density specified
8. Liquid propellant with initial mass of hydrazine, RP1 and liquid hydrogen plus initial temperature specified.
9. Solid rocket propellant, dense burning zone with initial diameter of zone, total area of propellant pieces, area multiplier for initial plume diameter and initial plume temperature specified

The input variable *amb_init* controls type of weather data inputs used:

1. Use linear temperature lapse profile & exponential pressure profile (not recommended)
2. Read input file with T, U, V, and P for nz axial heights, Z (default file = profile.dat)
3. Read input file from hysplit input (NAM format) (default file = nam.dat)

The discussion in Appendix A explains how input parameters *value1* through *value8* are used to accommodate the specification of required data for the above two variables

The input variable *ientrain* controls the entrainment model options

1. Entrainment Ve calculated using equation (10)
2. Entrainment Ve calculated using equation (11)
3. Entrainment Ve calculated using equation (25)
4. Input parameter *vent_min* specifies minimum velocity for entrainment (m/s)

The discussion in Appendix A explains how input parameters alpha1, *alpha2*, and *alpha3* are used to accommodate the specification of required data for *ientrain*.

The input variable *icondense* controls the condensation model when relative humidity exceeds 1.0:

1. *icondense* = 0 Model off
2. *icondense* = 1 Model on with condensed water vapor mass forming droplets which precipitate out of the puff
3. *icondense* = 2 Model On with-condensed wator vapor forming droplets that remain in the puff

The input variable *zinitial* specifies the initial elevation of puff (default = 0.0).

3 Titan 34D-9 Low-Altitude Explosion of April 18, 1986

On April 18, 1986, a Titan 34D rocket launched from Vandenberg Air Force Base. It aborted with a mid-air explosion 8.38 seconds after takeoff. The event was recorded by approximately orthogonal cameras, allowing for reasonable estimation of plume size and trajectory using photogrammetry [1 and 12]. The following discussion uses this analysis to compare measured results to IAT simulations. This is an important comparison for the IAT program because this software will be used to predict initial trajectory of particles after fires resulting from liquid rocket fuel combustion. Figure 5 contains a sequence of three photographs demonstrating the violence of the explosion. For reference, the explosion occurred at 253 meters above the launch pad.

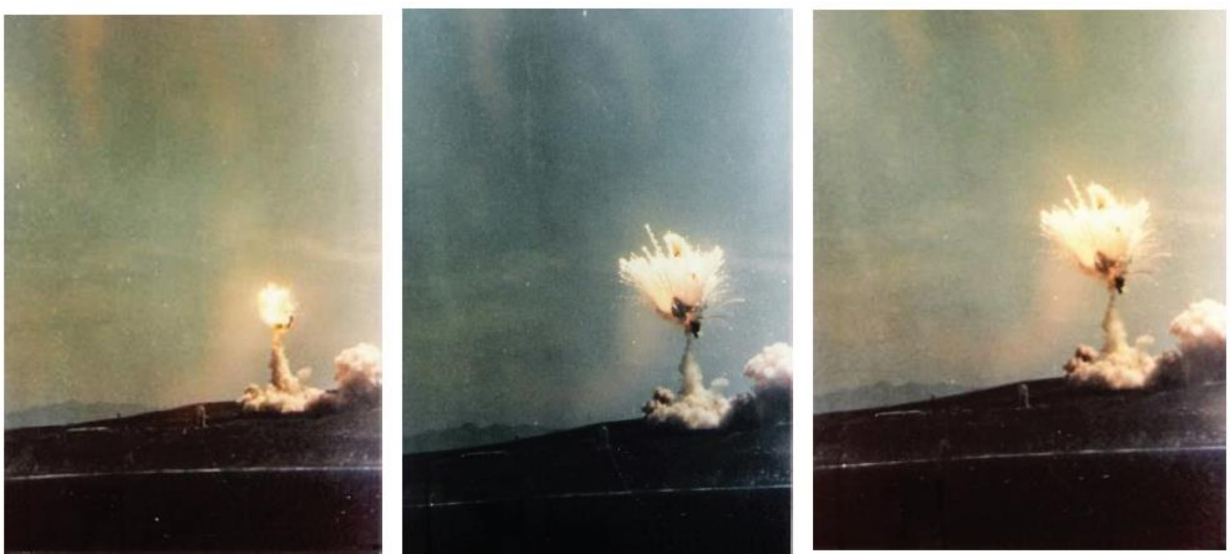

Figure 5: Titan 34D Explosion Sequence

3.1 Event Summary

Titan 34D-9 rocket lifted off at approximately 10:45 AM, PST. At 8.38 seconds after a seemingly normal launch, the rocket exploded. The A-50 fuel, a hypergol, ignited after the formation of a red cloud. This red cloud stands out in the photographs of Figure 6. It is particularly evident immediately after the accident. However, even after a considerable time, the vapor cloud remains tinged with red. The cloud's coloration is indicative of unconsumed nitrogen tetroxide the oxidizer carried by the Titan rocket.

Figure 6: Two Photographs – Immediately Following Explosion and Long Term

Explosion facts:

- Location: Launched from Latitude 34º37’55.3”N and Longitude 120º36’35.4”W.
- Abort Time: 8.38 seconds into launch
- Abort Elevation: 253 meters (830 ft.) above launch pad
- Launch pad SLC-4E elevation: 153 m (502 ft.).
- Total elevation above sea level: 406 m (1332 ft.)

Figure 7 contains an aerial photograph of the Vandenberg location taken eight years after the event. The elevation profile also included in the figure shows the launch pad at 153 m above sea level.

The Titan 34D used Aerozine-50 (A-50) for fuel. A-50 is a mix of 50% hydrazine (N_2H_4) and 50% unsymmetrical dimethylhydrazine, or UDMH ($H_2NN(CH_3)_2$). A-50 uses nitrogen tetroxide (N_2O_4) as an oxidizing agent. Table 6 contains a listing of the estimated initial fuel load for the launch.

Source: Google Earth

Figure 7: Aerial Photograph and Elevation Profile of SLC-4E Launch Site

Table 6: Fuel Load on Titan 34D [12]

	Aerozine-50	Ox	Total
Stage 1	103227	195164	298391
Stage 2	25038	44532	69570
Total (lb)	128265	239696	367961
Total (kg)	58180	108724	166904
O/F (kg/kg)	1.87		

These numbers represent the full cargo just prior to launch. The explosion occurred 8.38 seconds after launch and interim fuel consumption will have altered the cargo somewhat. However, the impact on subsequent calculations will be minor and is ignored.

3.2 Event Weather

The IAT code can use three types of weather data;

- Fixed thermal gradient (lapse rate) with stability class.
- IAT specific weather file.

- Data extracted using the North American Meteorology (NAM) data set. NAM data sets are available for dates from 2006 to current dates.

The first option offers limited utility and is not recommended by IAT authors. The second option is recommended if NAM data is unavailable, and is the option chosen to analyze the Titan 34D event. This accident occurred before the NAM database started.

Figure 8 contains plots of available weather data extracted from Dandini's (Sandia) letter of 11/23/1998 to Earl Wahlquist of the DOE [1]. Data is based on rawinsonde temperature profiles taken the day of the accident. The 10:15 profile was verified against data tabulated in [2].   Plots of temperature data are all dashed. The figure also contains a solid red curve which is an interpolation of temperature data to the time of the explosion. Subsequent IAT analyses in referred to in this paper used the data represented by this solid curve.

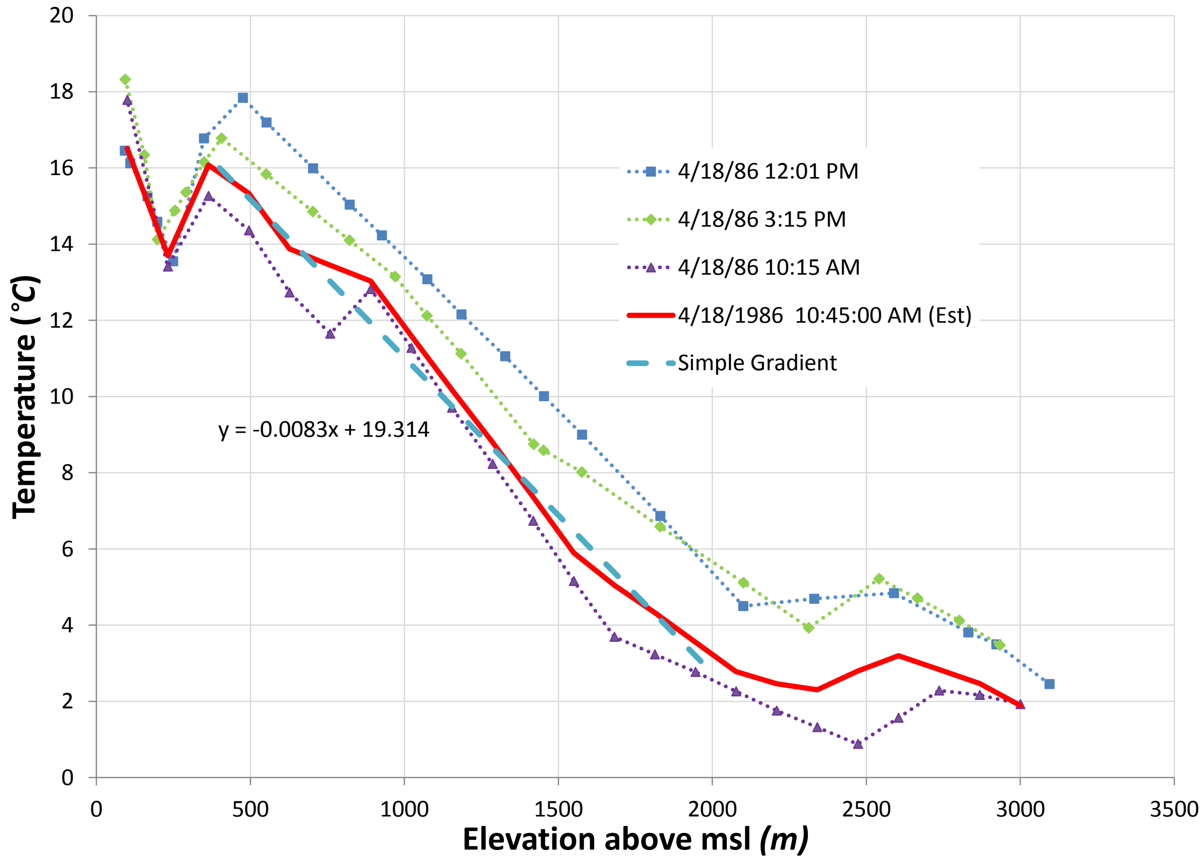

Figure 8: Temperature Profiles Taken at Approximately the Time of the Incident

Consider the straight dashed (blue) line in Figure 8. This line is a linear regression fit to the interpolated temperature data between 400 *m* (roughly detonation elevation) and 2000 *m* (roughly maximum puff height). The line's value is in demonstrating the overall thermal gradient during the time of the accident. The slope of this simple gradient line is -0.0083 K/m. This is indicative of a neutral Pasquale Stability Class.

Similarly Figure 9 contains plots of wind velocity data also extracted from the Dandini letter [1]. As before, the plotted data is based on rawinsonde profiles taken the day of the accident. Plots of velocity data are all dashed. Subsequent IAT analyses in this paper used the data represented here. The velocities and directions were reduced to directional components before inclusion in the weather file.

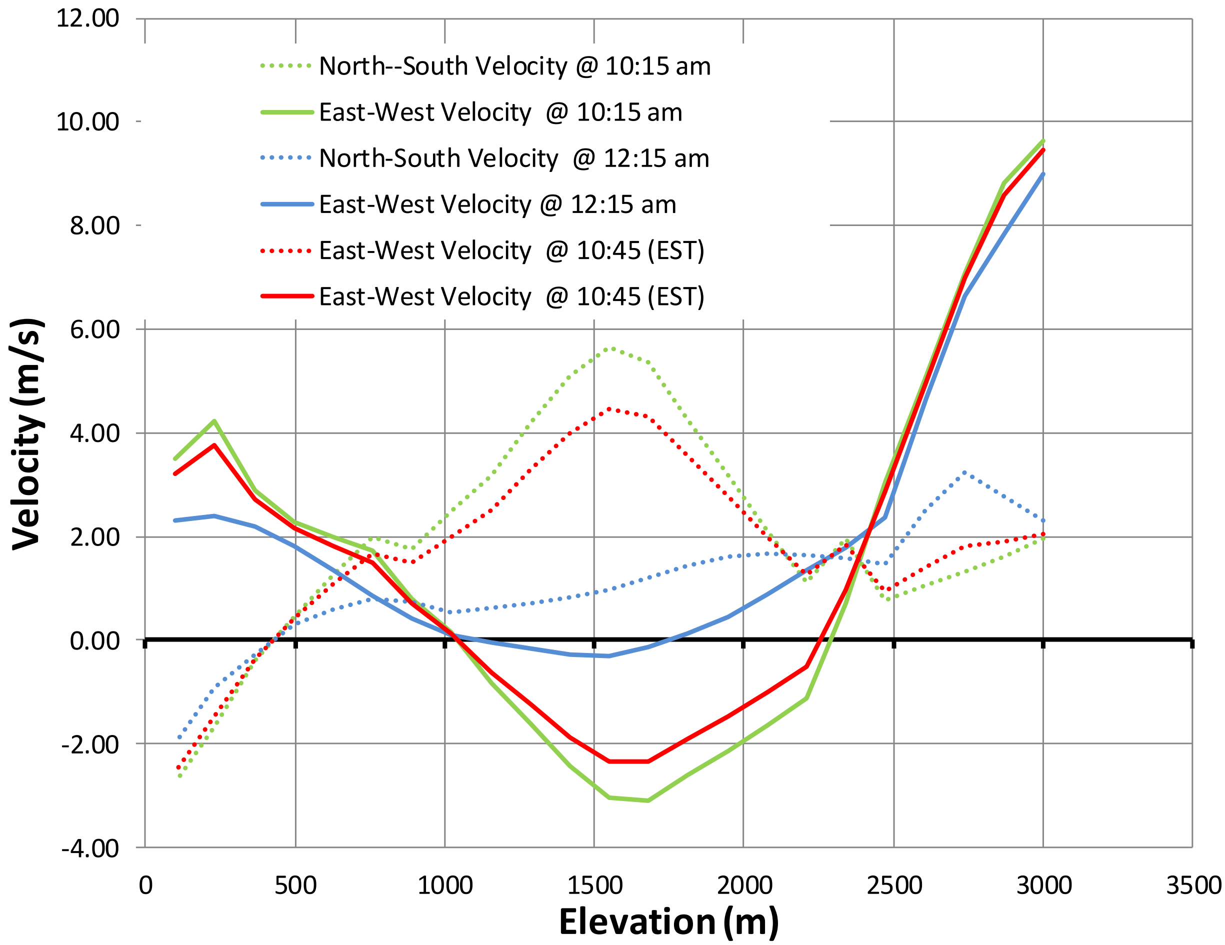

Figure 9: Wind Velocity Profiles Taken at Approximately the Time of the Incident

The appendix contains a listing to the data file used for these analyses.

3.3 Adaptation of IAT Inputs

As would be expected, comparison of the actual event to a model as simplified as is the IAT model requires some adaptation. The following is a discussion of the steps taken to accommodate any differences between reality and the environment that IAT can model.

3.3.1 Fuel and Fuel Mix

IAT runs made in support of this analysis assume the fuel is 100% hydrazine since IAT does not support A-50 as a fuel.

Physically, puff rise depends on the density of hot gas generated. Density depends in turn on puff temperature and molecular mass. Initial puff temperature is specified as an input and subsequently, puff temperature is calculated based on entrainment and radiation. The plume is in pressure equilibrium with the atmosphere; the pressure profile is an input via weather data. This leaves molecular mass as the outstanding variable

With regard to molecular mass, Table 7 contains lists of products generated with concentrations during combustion of each of three fuels, hydrazine, UDMH and A-50. All fuels were assumed to burn with pure oxidizer, and oxidizer/fuel ratios were adjusted so that all three fuels' initial temperature was equal to the base case initial temperature of 2700 K. This data was used to calculate molecular mass. Molecular mass of hydrazine combustion products was within 4.2% of A-50. In fact, the molecular mass used for IAT analyses was 20 kg/kmol, slightly higher than calculated in the table, to allow for combustion with some air and at other temperatures.

Table 7: Products Molecular Mass for Three Fuels at 2700 K

Species	Component Molecular Mass	UDMH	Hydrazine	Aerozine-50
		$CNN(CH_3)_2$	N_2H_4	50% Hyd/50% UDMH
CO	28.0101	0.188206	3E-07	0.117476
CO_2	44.0095	0.044893	0	0.020182
COOH	45.0174	2E-07	0	-
H	1.00794	0.040869	0.027308	0.027911
H_2	2.01588	0.161237	0.230241	0.238961
H_2O	18.0153	0.273336	0.343384	0.276051
H_2O_2	34.0147	2E-07	0	-
HCO	29.018	7E-07	0	4E-07
HNO	31.014	4E-07	2E-07	2E-07
HO_2	33.0067	1.8E-06	5E-07	3E-07
N	14.0067	2.8E-06	0.000001	9E-07
N_2	28.0134	0.26129	0.385353	0.308754
NH	15.01464	7E-07	4E-07	4E-07
NH_2	16.02258	3E-07	3E-07	3E-07
NH_3	17.03052	3E-07	6E-07	6E-07
NO	30.0061	0.002357	0.001055	0.000735
NO_2	46.0055	2E-07	0	-
O	15.9994	0.003234	0.000784	0.000612
O_2	31.9988	0.002188	0.000472	0.000285
OH	17.00734	0.022383	0.011399	0.009031
	Products Molecular Mass	**20.4308**	**17.7261**	**18.5056**

The data of Table 7 was generated using the RPA standard edition computer code v.1.2.6.[13]

3.3.2 Initial Temperature

The IAT cases run for this analysis assume for a base case an initial temperature of 2700 K. This is equivalent to assuming half of the fuel burns using oxidizer and half burns in air and that combustion occurs with fuel/oxidizer mixtures that very nearly maximize temperature.

Figure 10 provides plots of adiabatic flame temperature versus oxidizer excess coefficient, a measure of the departure from stoichiometric for the combustion reaction. An assumption of adiabatic flame temperature for the first seconds after an accident is realistic as insufficient time has elapsed to allow for any significant heat transfer. The curves in Figure 10 were generated using the RPA code. [13]

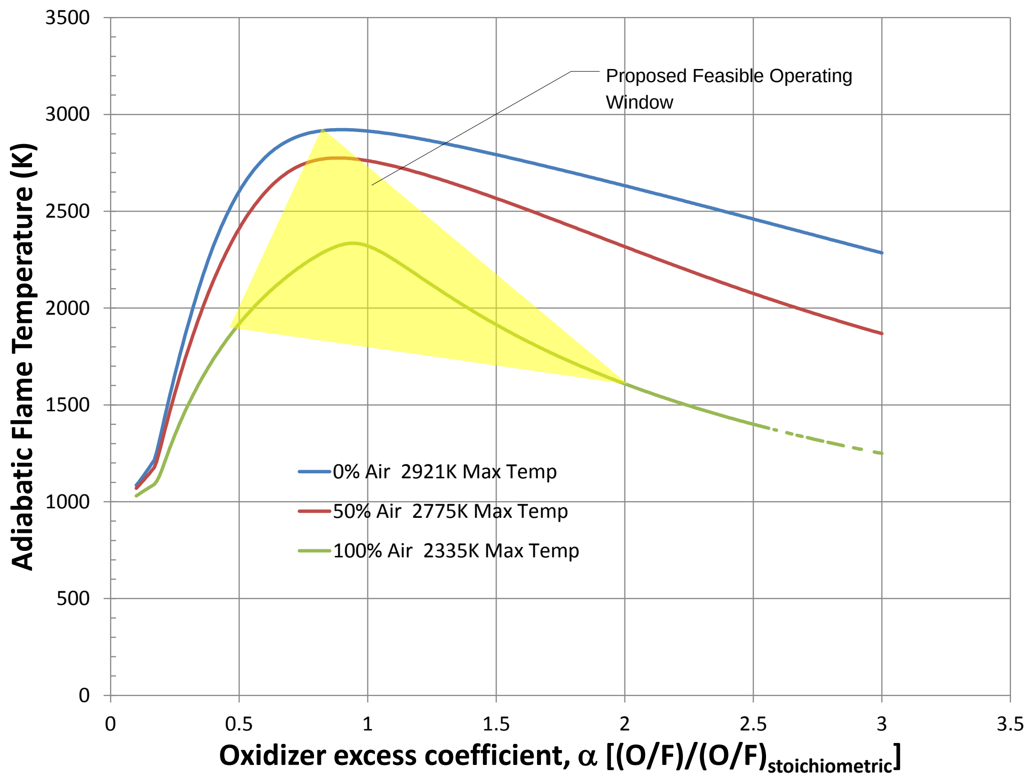

Figure 10: Adiabatic Flame Temperature Various Oxidizer Mixes

In the event that combustion occurs in 100% air, the lowest of the three curves in Figure 10 would apply. Given the availability of air, one can postulate extremely high α ratios for combustion in air. However, given the hypergolic nature of the fuel, it is unlikely that excessively lean environments would occur. The mixture would ignite before that occurs. This would limit maximum α to a relatively low number, arbitrarily assumed to be 2.0 for this exercise. In fact, the fuel would probably dump as a contiguous cloud with air migrating inward from the edges of fuel cloud. This would argue for a rich environment with α less than one. For this exercise, the lower limit of α was arbitrarily assumed to be 0.5. This discussion provides the basis for the operating envelope sketched in Figure 10.

Based on the above discussion, initial temperatures can range from 1620 K to 2920 K. Section 3.6.2 includes a discussion of the sensitivity of puff trajectory results to this range of temperatures. That discussion will demonstrate a significant lack of sensitivity.

3.4 Titan 34D Simulation Base Case

In lieu of an extensive input deck or text file, the IAT code asks for a sequence of input parameters as a command line. Table 8 contains a listing of these IAT inputs that were used for the Titan 34D validation runs. The parameters listed in bold type in Table 8 will be involved in sensitivity studies later.

Table 8: IAT Command Line Inputs – Base Case

Code Variable Name	Description	Value	Units
puff_init	Puff Model Selector	8	--
amb_init	Atmosphere Profile Model Selector	2	--
value1	Mass of RP-1 Fuel	0	kg
value2	Mass of Liquid Hydrogen Fuel	0	kg
value3	Mass of Hydrazine	58180	kg
value4	not used	0	
value5	not used	0	
value6	not used	0	
value7	not used	0	
value8	**Initial Puff Temperature**	2700	K
ientrain	Entrainment Type	3	--
alpha1	**entrainment coeff. (vertical velocity)**	0.15	--
alpha2	**entrainment coeff. (lateral velocity)**	0.15	--
alpha3	**entrainment coeff. (turbulent)**	0.65	--
vent_min	Threshold velocity below which entrainment is turned off	0.1	m/s
icondense	Water Condensation Model.	2	--
z_zero	Detonation altitude	405	m

A value of 8 for the *puff-init* variable specifies that the event will be a liquid burn and that variables *value1*, *value2*, and *value3* designate fuel or oxidizer masses. Selection of *puff-init* = 8 also specifies that *value8* will contain the initial puff temperature.

A value of 2 for the *amb_init* variable specifies that the code should use a weather file, *profile.dat*, containing temperature, horizontal velocities and pressure as a function of height above a datum. The file *profile.dat* conforms to the non-NAM IAT format for weather data. Refer to the appendix of a listing of *profile.dat*.

A value of 3 for the *ientrain* variable specifies that the code will be using a three-variable entrainment model as described in detail in Section 3.6.1. As a result, the code looks for non-zero values of variables *alpha1*, *alpha2* and *alpha3*. In addition, the code looks for a value for variable *vent_min*. This variable identifies a velocity above which entrainment is active.

3.5 Results

Figure 11 contains a plot of IAT predicted plume elevation versus time using base case inputs. The figure contains as background a plot based on photogrammetric results from the incident plotted to the same range of time and elevation. This overlaying of results allows direct comparison of the two data sets. The original plot was taken from the Abernathy report [12]. The plume top height, middle, and bottom heights are shown as solid lines. Also included on this plot are the photometric measurements of the puff diameter as a function of time shown as black dashed lines. The background shows two orthogonal dimensions.

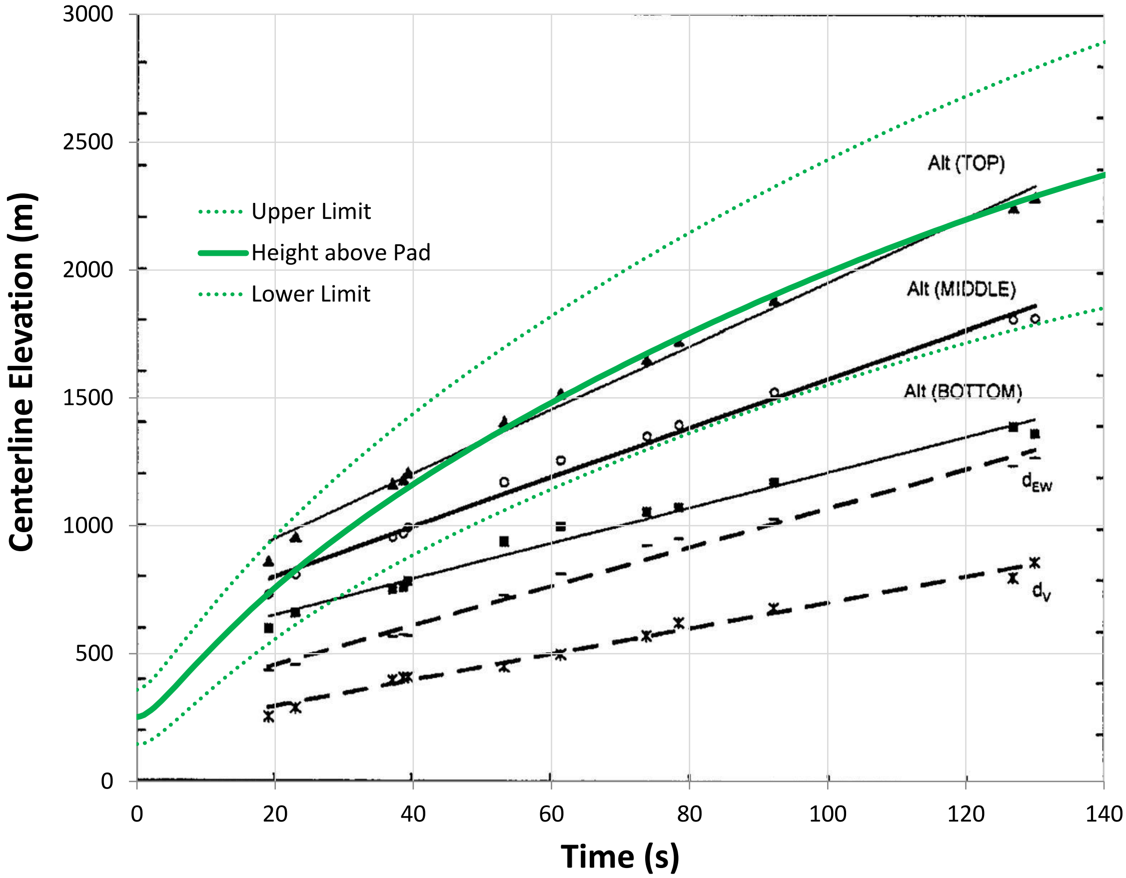

Figure 11: Base Case Plume Centerline and Elevation Prediction

The IAT predictions (green lines for the plume top, centroid, and bottom) are slightly higher than measured data for the event. In addition, the IAT predictions exhibit more curvature than exhibited by the photogrammetric results for the original report. Abernathy plots the trajectory as a straight line. His data, however, does indicate some slight curvature. The use of a linear fit is probably reasonable given his projected measurement accuracy. However, a linear fit does not appear physically reasonable. For example, extrapolation back to time zero would indicate the explosion would have to occur much higher than it actually did.

At this point in the exercise, several runs were made varying the single parameter alpha1 (the entrainment coefficient for the vertical velocity contribution*)*. As discussed in Section 3.6 puff height is most sensitive to this parameter. The results are shown in Figure 12.

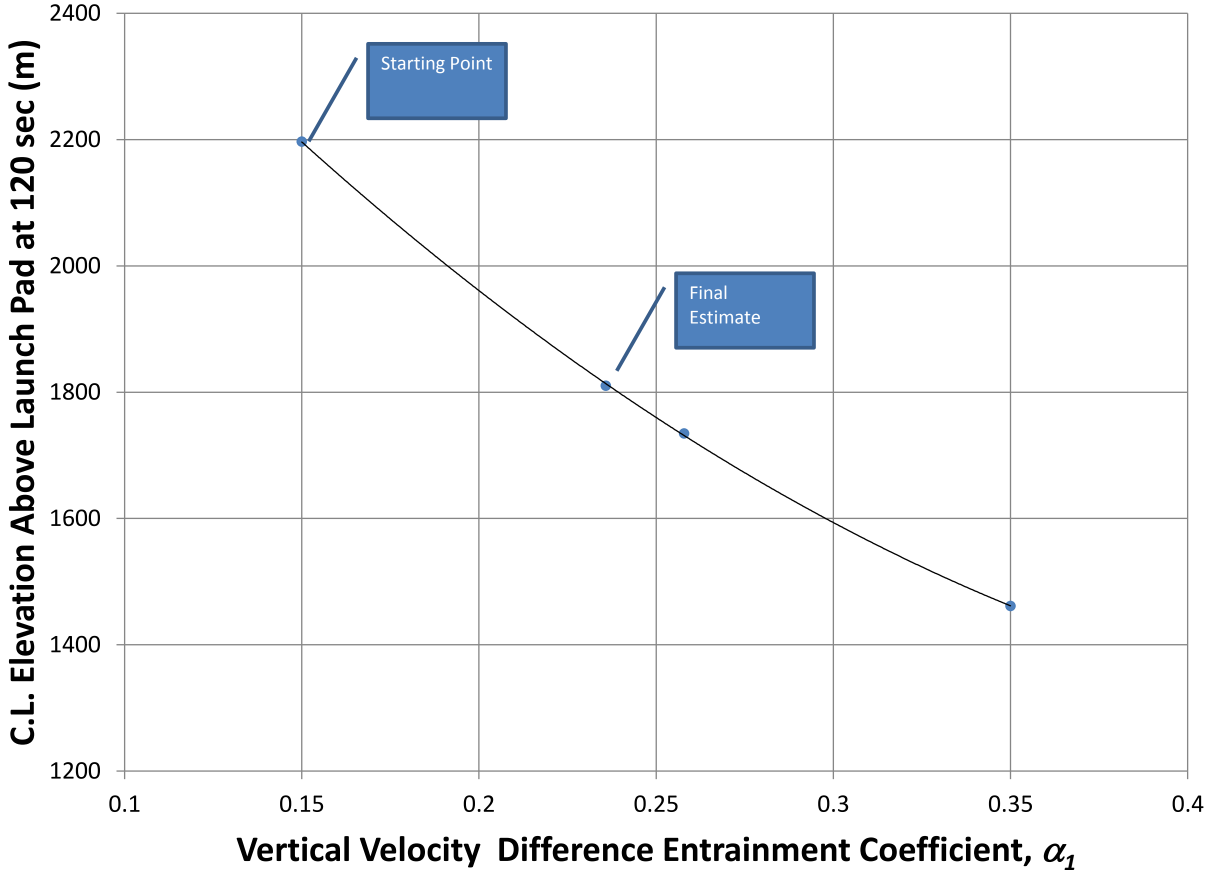

Figure 12: Dependence of Puff Height on α_1

Based on Figure 12, the value of $\alpha_1 = 0.24$ calibrates IAT best to the observed results. This is well within the range of reasonable values for this parameter (literature values range from 0.15 to 0.5) [1, 2]. A plot of IAT results keeping everything else constant and using $\alpha_1 = 0.24$ is shown in Figure 13. As before, the figure contains the original plot of plume trajectory as background.

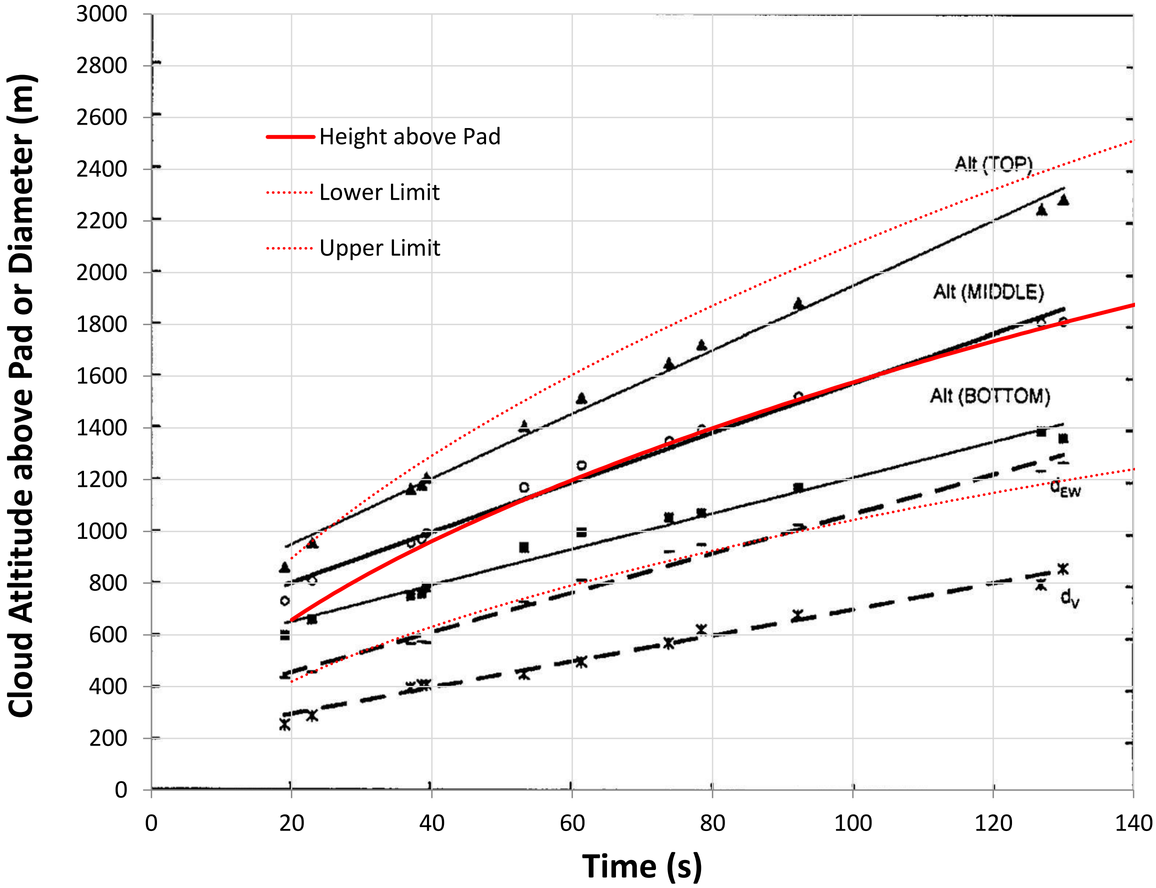

Figure 13: Cloud Centerline Elevation α_1 Coefficient increased to 0.24

The resulting IAT prediction agrees well with measured trajectory data from the accident. This agreement is particularly true if one looks only at the original data points and not the straight line Abernathy fit to the data. More discussion on this agreement and its implications occurs below during the rate of rise comparisons.

IAT tends to over-predict puff dimension. This over prediction is indicated by the discrepancy between Abernathy's top or bottom elevation lines and the similar lines for IAT, labeled Upper or Lower Limit (red dashed lines). Differences between the photogrammetry and IAT simulation are to be expected as the code and the Abernathy report use different criteria to establish the limits. IAT assumes that composition is constant across the puff (OD approximation) and calculates the dimension based on puff temperature, pressure, and mass including entrainment. The Abernathy report relied on visible edges of the cloud to determine limits. With these differences in mind, the IAT predictions come remarkably close to the measured limits.

Figure 14 furthers this discussion of puff diameter. The figure contains the same Abernathy plot as background; this plot contains two dashed black lines which are the east-west (lateral) dimension and vertical puff dimension as a function of time. The graph also shows IAT's prediction of a puff spherical diameter as a solid red line. This prediction is for the same calibrated IAT case as plotted in Figure 13. Again, the IAT prediction is slightly higher than the measurements. As above, the IAT predictions are remarkably close when one considers the different methods each plot used to determine the limits.

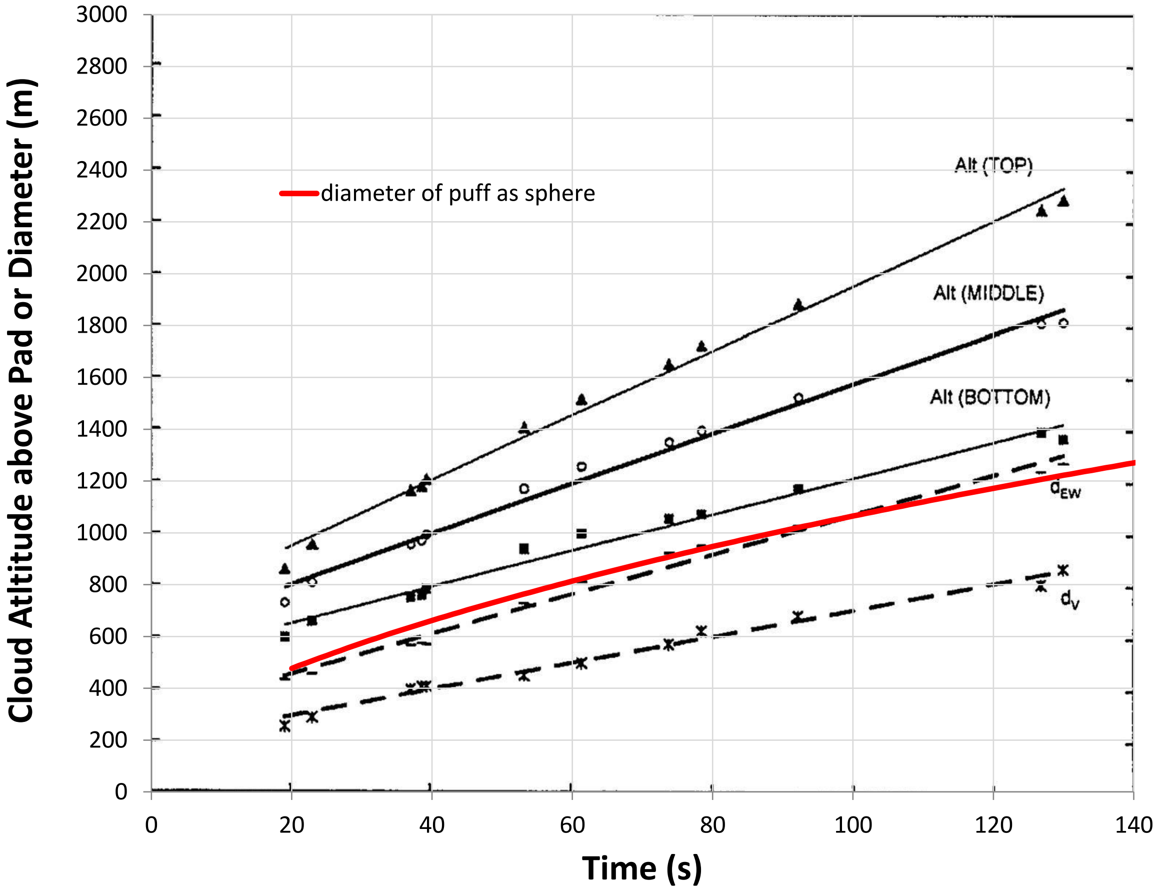

Figure 14: Puff Diameter

Figure 15 contains a plot of equivalent sphere volume for the same IAT run plotted in Figure 13 and Figure 14 ($\alpha_1 = 0.24$). For this plot, the solid black line is an experimental estimate of volume based on non-spherical dimensions; the solid blue line is the IAT predicted volume using its spherical assumption. As would be expected based on previous discussion, the level of agreement is quite good. Equally important is the parallelism exhibited between the IAT simulation and the background curve. This parallelism indicates that IAT's treatment of entrainment (after calibration) is adequate.

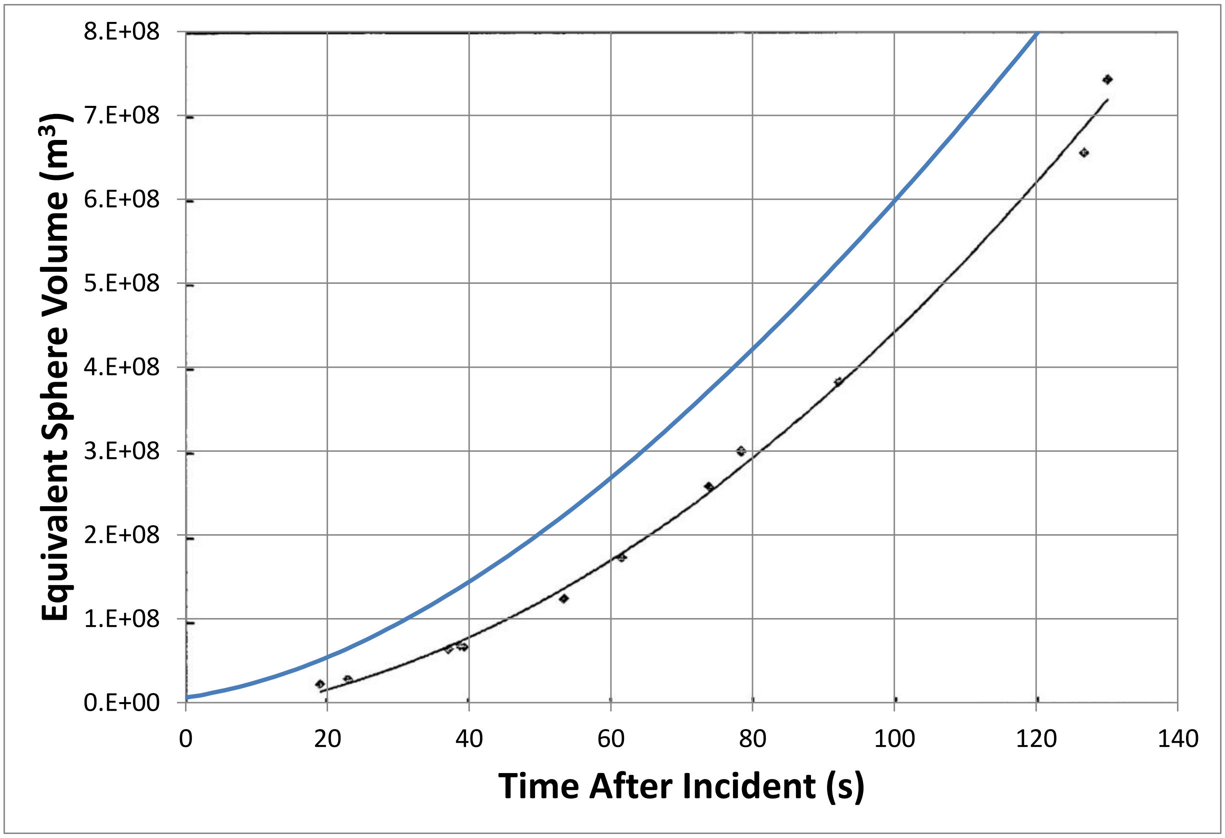

Figure 15: Equivalent Sphere Volume

Figure 16 introduces another interesting validation point. The figure consists of a graph containing as background the elevation versus photogrammetry plot used in previous graphs. In this case, the actual data points were identified with crosses (in green). These points were then fit to a power law curve. This form of analytic expression was chosen in lieu of the straight linear form chosen by Abernethy [12] because it better reflects the physics of puff rise. For example, this analytic form captures early time departures from a straight line. It also generates non-trivial derivatives. The fit has the form:

$$z = 172.86t^{0.4803} \qquad 1$$

Figure 16 shows as dotted lines the 95% confidence boundaries for this fit. The equation predicts the centerline elevation of the puff.

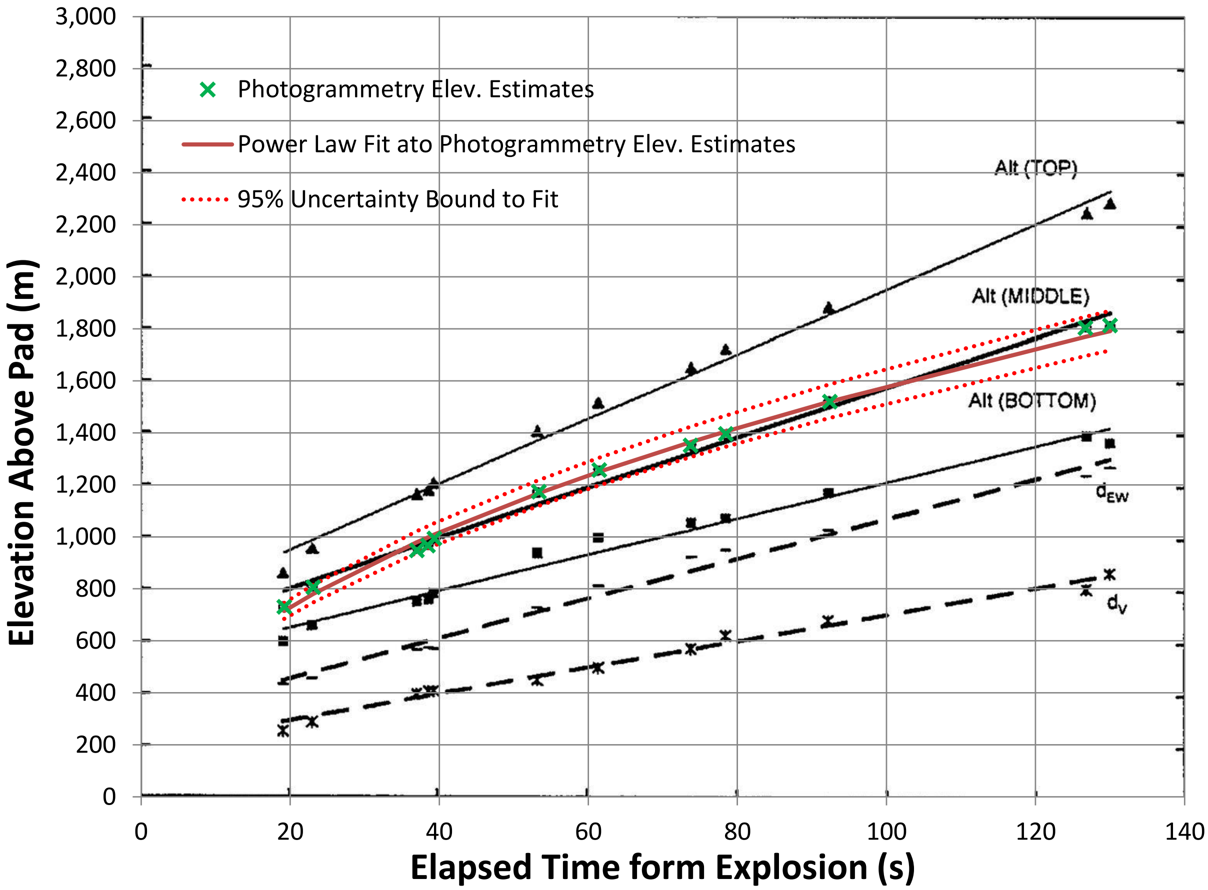

Figure 16: Power Law Fit to Photogrammetry Data

Figure 17 shows a remarkable plot based on the power law fit described above which argues most strongly for validation of the IAT code. The power line fit describes a non-linear elevation versus time trajectory. Its derivative, the short (green) line in Figure 17, is a plot of vertical velocity versus time based on photogrammetric results. The measured data does not capture early time (t < 20 s) dynamics.

Sandia's IAT code also outputs vertical velocity as a function of time. This output is plotted as the more extensive (red) line in the plot. The IAT plot is based on the same inputs used to obtain the graph plotted in Figure 13. This IAT plot is appears physically realistic. The puff starts out hot and is, as a consequence, highly buoyant. This initial buoyancy provides a strong acceleration during the first approximately 10 seconds. However, as will be shown in Section 3.6, the thermal driver for buoyancy drops off rapidly. With cooling, the plume's vertical velocity slows. Again, this behavior is all reasonable.

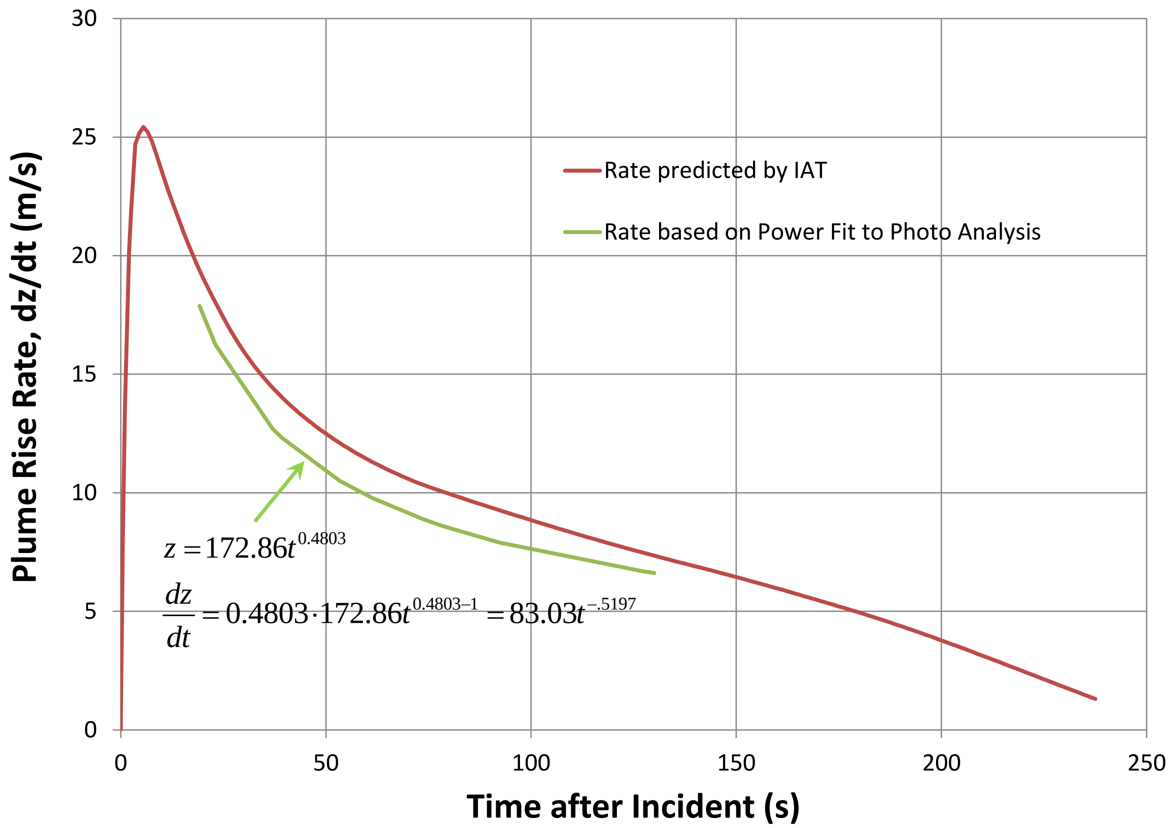

Figure 17: Puff Rate of Rise

Within approximately 20 seconds, the two lines are parallel and are almost coincidental. This level of agreement argues that IAT has captured the physics involved in at least the long term rise period. The fact that IAT also reasonably predicts actual elevation indicates that it has captured the physics of initial rise also.

3.6 Sensitivity Cases Run

This section contains descriptions of the sensitivity analyses conducted with IAT to determine the overall sensitivity of the results shown to input parameters. The sensitivities were run on the parameters shown in bold font in Table 8. The number of sensitivities and the details of these sensitivities are shown in the following discussion.

All sensitivities were conducted relative to the base case described in Section 3.4.

3.6.1 Entrainment Sensitivities

Entrainment in IAT is determined via equation 9. The three α's in equation 9 constitute the primary source of uncertainty and are used here to determine sensitivity. These three parameters can vary between 0 and 1 and are empirical, containing only a loose relationship to physical phenomena. For sensitivity, each of the three alpha parameters was incrementally changed between 0.15 and 1, resulting in 27 IAT runs, each of which is listed in Table 9.

Table 9: List of Entrainment Sensitivity Cases Run

Case ID	α1	α2	α3
α1–1	0.15	0.15	0.65
α1-2	0.25	0.15	0.65
α1–3	0.35	0.15	0.65
α1-4	0.45	0.15	0.65
α1–5	0.55	0.15	0.65
α1-6	0.65	0.15	0.65
α1–7	0.75	0.15	0.65
α1-8	0.85	0.15	0.65
α1–9	0.95	0.15	0.65
α2–1	0.15	0.15	0.65
α2-2	0.15	0.25	0.65
α2–3	0.15	0.35	0.65
α2-4	0.15	0.45	0.65
α2–5	0.15	0.55	0.65
α2-6	0.15	0.65	0.65
α2–7	0.15	0.75	0.65
α2-8	0.15	0.85	0.65
α2–9	0.15	0.95	0.65
α3–1	0.15	0.15	0.15
α3-2	0.15	0.15	0.25
α3–3	0.15	0.15	0.35
α3-4	0.15	0.15	0.45
α3–5	0.15	0.15	0.55
α3-6	0.15	0.15	0.65
α3–7	0.15	0.15	0.75
α3-8	0.15	0.15	0.85
α3–9	0.15	0.15	0.65

The results from these sensitivities are plotted in Figure 18.

These IAT runs exhibit effectively no relationship between plume elevation and the alpha2, or α_2, parameter. This is to be expected. The puff accelerates to the ambient horizontal velocity almost immediately. Without a shear between the puff and horizontal velocity, little or no entrainment occurs via this mechanism.

The alpha3 parameter relates entrainment to turbulent kinetic energy or TKE. Unlike the alpha 2 parameter, one would have expected more impact from the alpha3, or α_3, parameter values. A weak correlation exists between alpha3 and puff height, but it is too weak to consider this parameter a major contributor to puff height variation. One explanation for the weak correlation is that the accident occurred in stable air and TKE is too small to exert much impact on the overall puff performance.

The major driver among entrainment parameters for the liquid propellant plume is the vertical velocity parameter alpha1, α_1. This is as would be expected. The extremely high initial velocity exhibited in Figure 17 would indicate significant overrun between the puff and ambient air resulting in a lot of entrainment.

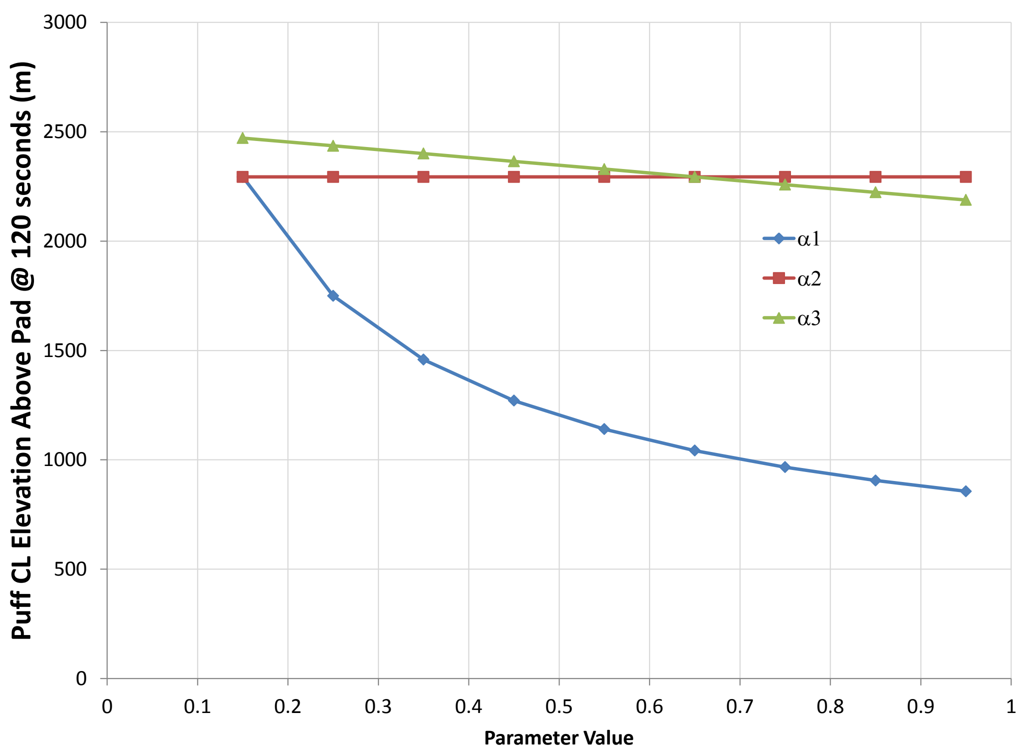

Figure 18: Sensitivity of Plume Elevation to Entrainment Parameters Variation

3.6.2 Initial Puff Temperature Sensitivity

As discussed in Section 3.3.2 puff initial temperature could vary between 1500 K and 2700 K depending on degree of mixing with air. To determine strength of the relationship between this parameter and puff height, nine sensitivities were run. The nine sensitivities are listed in Table 10 along with the control line inputs for each.

Table 10: List of Initial Temperature Sensitivity Cases

Case ID	Initial Temperature
T0-1	1500
T0-2	1700
T0-3	1900
T0-4	2100
T0-5	2300
T0-6	2500
T0-7	2700
T0-8	2900
T0-9	3100

Figure 19 contains a plot that illustrates the results of these sensitivities. As the figure shows, only a weak correlation exists between initial puff temperature and plume height.

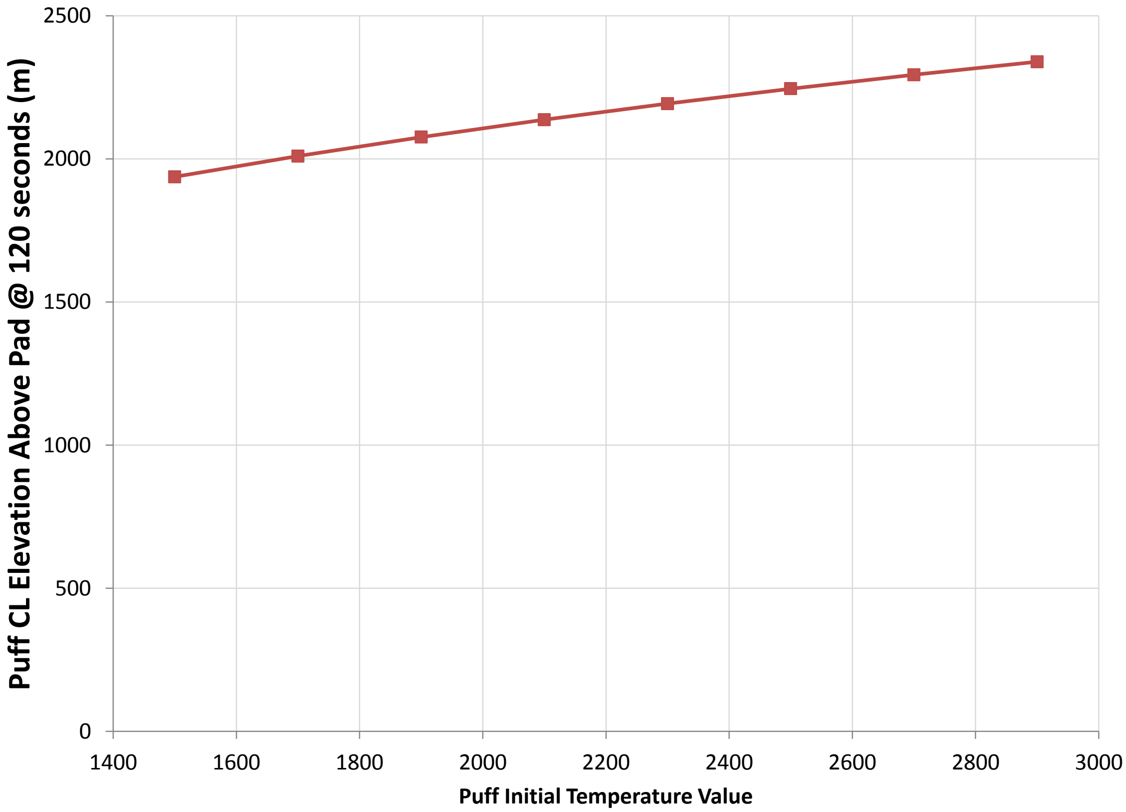

Figure 19: Sensitivity of Plume Elevation to Puff Initial Temperature

After some thought, this lack of strong correlation is to be expected. Look at Figure 20, a plot of puff temperature with time. Entrainment cools the puff extremely quickly. As such, differences in initial puff temperature don't have that much time to work on the puff rise.

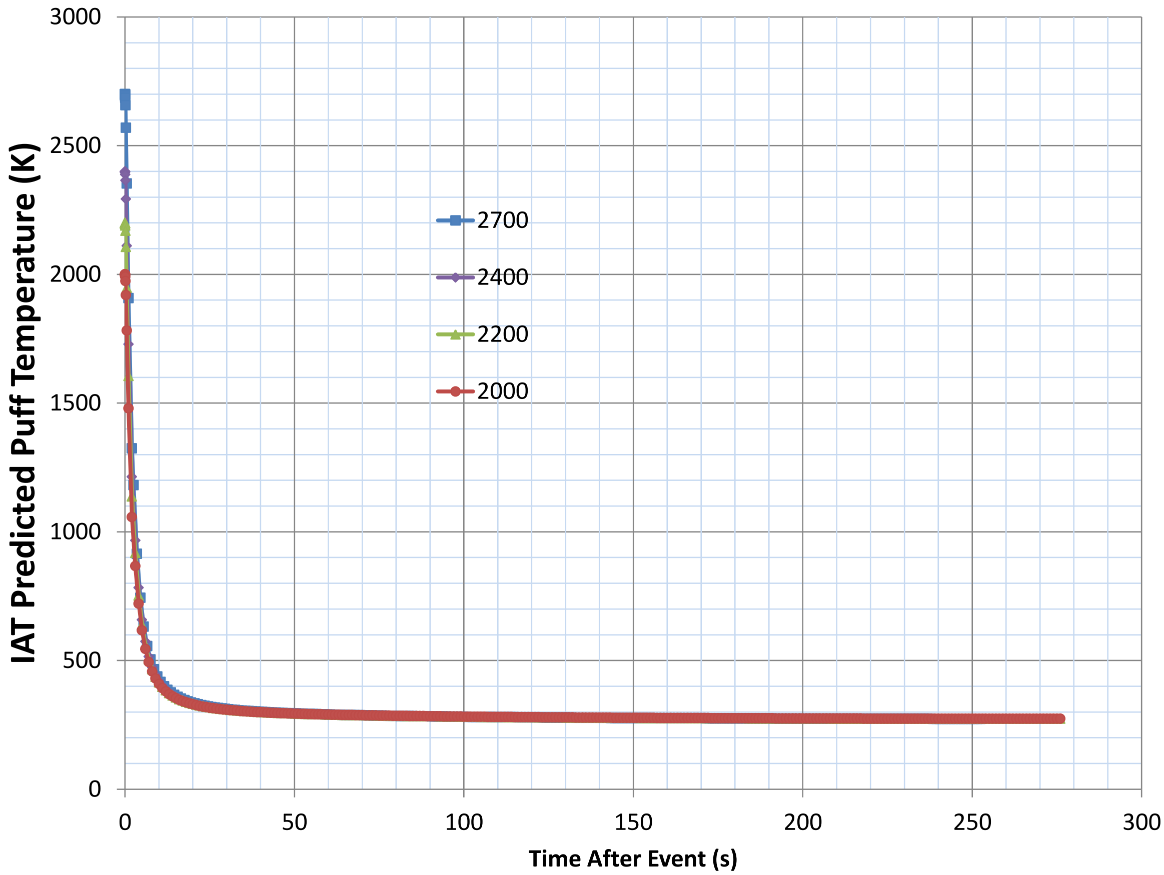

Figure 20: Initial Puff Temperature Impacts Only the First 10 seconds

Figure 21 provides further insight. The data in this new figure is identical to the previous. In this figure, however, the x-axis is now logarithmic, accentuating the initial seconds. One can see that below about 0.1 s, temperature differences manifest themselves. However, within 1 second from detonation, initial temperature differences are effectively mitigated. Within 10 seconds, temperatures trajectories have converged to the same temperature.

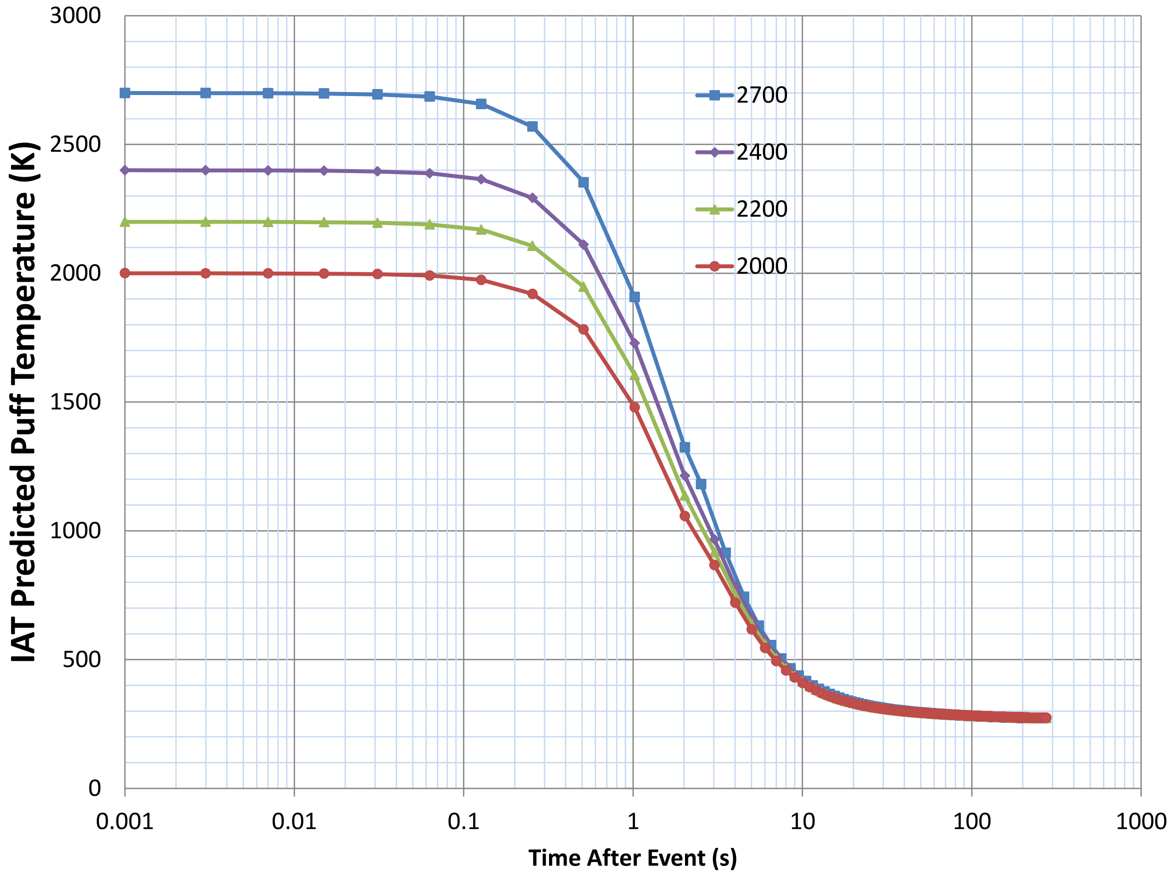

Figure 21: Initial Puff Temperature Impacts Only the First 10 seconds [2]

4 APL 2012 Solid Propellant Tests

The Johns Hopkins University Applied Physics Laboratory (JHU/APL, or simply APL) performed a series of open-air burns of solid propellant at the Alliant Technology (ATK) burn site in Elkton, MD in June of 2012. The plumes from these burns were photographed using digital video cameras. The APL tests consisted of several burns, each involving solid rocket propellants. Two of the large propellant block burns were conducted on large blocks of concrete and one on a metal surface coated with FlexFram. In all three of these large propellant block cases, the burning occurred on the bottom surface and the side surfaces. The burns occurred on a raised platform about 1 m above the ground and 8 ft (2.4 m) in diameter. Refer to APL's test report [16] for details of the tests. Subsequently, the SNL memo by Gelbard and Lipinski [16] provided estimates of the peak plume rise for the three burns. Appendix B contains the memo; Table 11 was extracted from that memo. This table contains the plume height estimates.

Table 11: Sold Burns Maximum Plume Height (Top of Plume) Estimates [16]

	Camera #1	**Camera #2**
June 5, 2012	146 ft ± 30 ft. (45 m ± 9 m)	207 ft ± 30 ft. (63 m ± 9 m)
June 6, 2012	256 ± 40 ft. (78 m ± 12 m)	276 ± 40 ft. (84 m ± 12 m)
June 7, 2012	138 ± 20 ft. (42 m ± 6 m)	malfunction

The three burns analyzed occurred on three consecutive days between June 5 and June 7 of 2012.

Figure 22 contains a photograph of a typical burn. This photo was taken during the test of 6/5/2012. Notice the characteristics of the plume with its initial rapid rate of rise combined with slight dispersion followed by a slower rise combined with a more significant dispersion. Typically, IAT computes the centerline elevation at the end of the rapid rise rate phase and leaves dispersion and dispersion/distribution to other codes in the Sandia suite. However, for this calibration/validation exercise, IAT was allowed to run out to times that match the times used in the photogrammetric analysis.

4.1 IAT Input

4.2 Solid Rocket Propellant Base Case

All three burns were of the same size and energy. The only variable was weather. As a consequence the same IAT command line was used for each burn, each using a different NAM file. The IAT command line was:

```
IAT 5 3 0.5  2600. 25.  0. 0. 0. 0. 0.  3 0.25 0.15 0.30 0.2 2 00.0
```

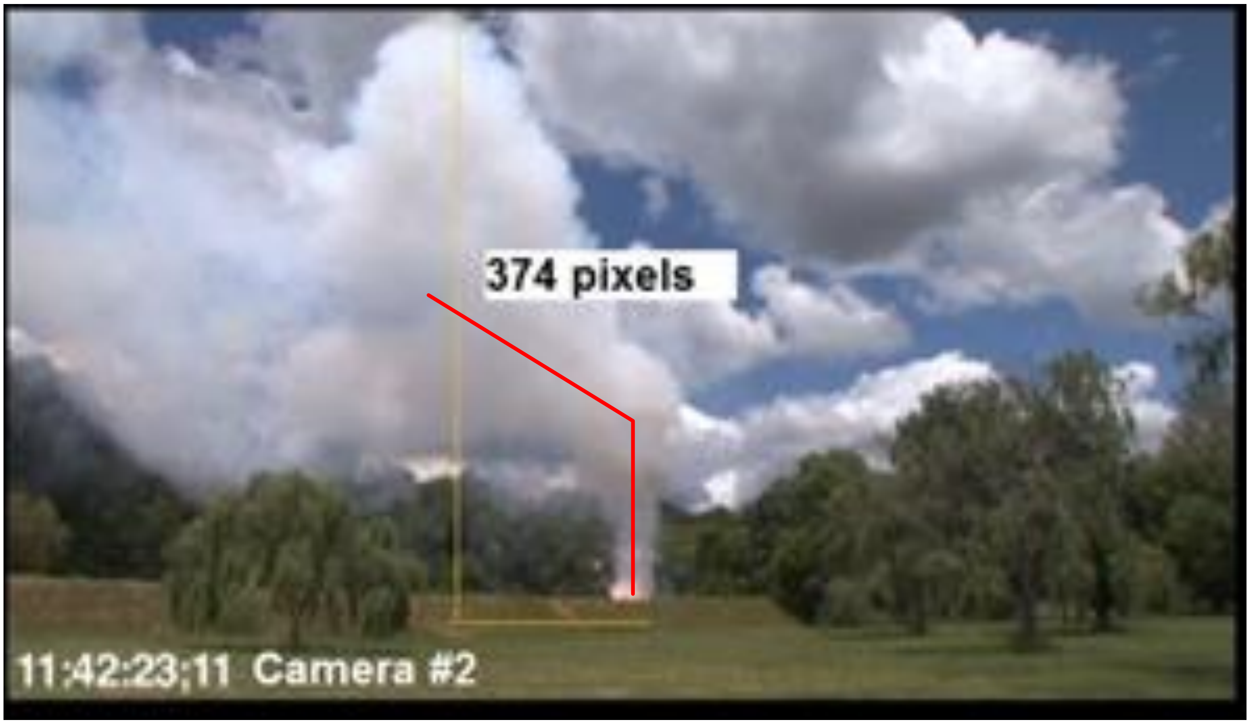

Figure 22: Typical Solid Propellant Burn with Plume

Details of the IAT command line are shown in more detail in Table 12 and explained in the following discussion.

A value of 5 for the *puff-init* variable specifies that the event will be a solid burn and that variables *value1*, *value2*, and *value3* designate propellant diameter, initial puff temperature and area multiplier (used only for multiple propellant sources) respectively.

A value of 3 for the *amb_init* variable specifies that the code should use a NAM weather file, *nam.dat*. Refer to the appendix of a listing of the three *nam.dat* files used in this analysis.

A value of 3 for the *ientrain* variable specifies that the code will be using a three-variable entrainment model as described in detail in Section 3.6.1. As a result, the code looks for non-zero values of variables *alpha1*, *alpha2* and *alpha3*. In addition, the code looks for a value for variable *vent_min*. This variable identifies a velocity above which entrainment is active.

The parameter *icondense* specifies IAT's treatment of water condensate in the cloud. With a value of 2, as used here, water will be allowed to condense but the small droplets will continue to propagate with the plume.

The solid propellant burn occurs at ground level, 0.0 m above the datum.

Table 12: IAT Command Line Inputs – APL Solid Burn

Code Variable Name	Description	Value	Units
puff_init	Puff Model Selector	5	--
amb_init	Atmosphere Profile Model Selector	3	--
value1	Initial diameter of right circular propellant fragment	0.5	m
value2	Initial Puff Temperature	2600	K
value3	Area multiplier	25	
value4	not used	0	
value5	not used	0	
value6	not used	0	
value7	not used	0	
value8	not used	0	K
ientrain	Entrainment Type	3	--
alpha1	entrainment coeff. (vertical velocity)	0.25	--
alpha2	entrainment coeff. (lateral velocity)	0.15	--
alpha3	entrainment coeff. (turbulent)	0.3	--
vent_min	Threshold velocity below which entrainment is turned off	0.2	m/s
icondense	Water Condensation model	2	--
z_zero	Detonation altitude	0.0	m

4.3 Weather

Six weather data files used in this solid propellant burn analysis are contained in Appendix B. These files were downloaded from the North American Meteorology (NAM) historical weather database. This analysis used two weather sets per day to bracket the time of the actual test.

Temperature gradients with elevation are plotted for each of the six weather files in Figure 23. The gradient for all of the six days is fairly consistent, averaging -0.0105 K/m for the six between ground and 1000 m. For reference, this corresponds to a neutral Pasquale-Gifford turbulent class.

It is interesting that temperatures rose continuously from June 5 through June 7. They started out at 19.5 °C (67.1 °F) at noon on June 5 and ended at 25.6 °C (78.1 °F) at 3:00 PM on June 7.

Although it has not yet been quantified, the use of NAM weather data files can impose some uncertainty to the IAT estimate. The NAM database covers all of North America. Weather for specific locations is interpolated from nodes closest to that spot.

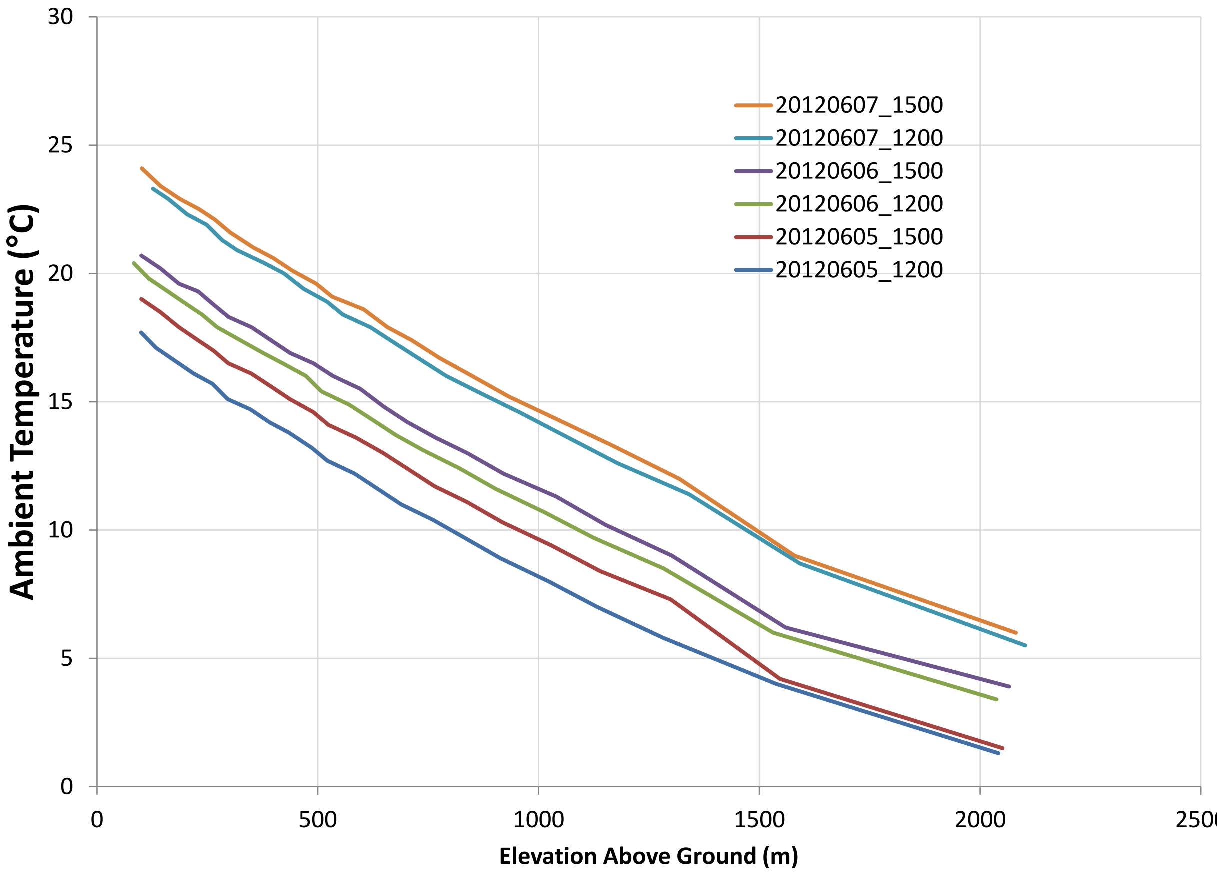

Figure 23: Temperature Plot against Elevation for Size Weather Files

4.4 Results for Solid Burns

In general, IAT simulations matched well the measured plume heights. For the first two days, June 5 and 6, IAT simulations matched measured top of plume fairly well. On the third day, the IAT code slightly over-predicted plume rise.

See Figure 24 for a summary of the comparisons. This figure takes some explaining. The two crosshatch patterns identify the two cameras used for photogrammetric analysis. In the case of the cross-hatched areas, width has no significance. The height of the crosshatch patterns is proportional to estimate uncertainty. In this case, uncertainty estimates were subjective and reflect the analyst's best guess at a single standard deviation. The figure shows only the single standard deviation for the estimates. Inclusion of two or three standard deviations would show significant overlap between estimates for a given day. Each date also shows two dark dots. This duality denotes IAT simulations of top of plume in meters using two weather data files extracted from the NAM database available for that date. The timing of the weather files bracket the time of the test. The dots denote plume top.

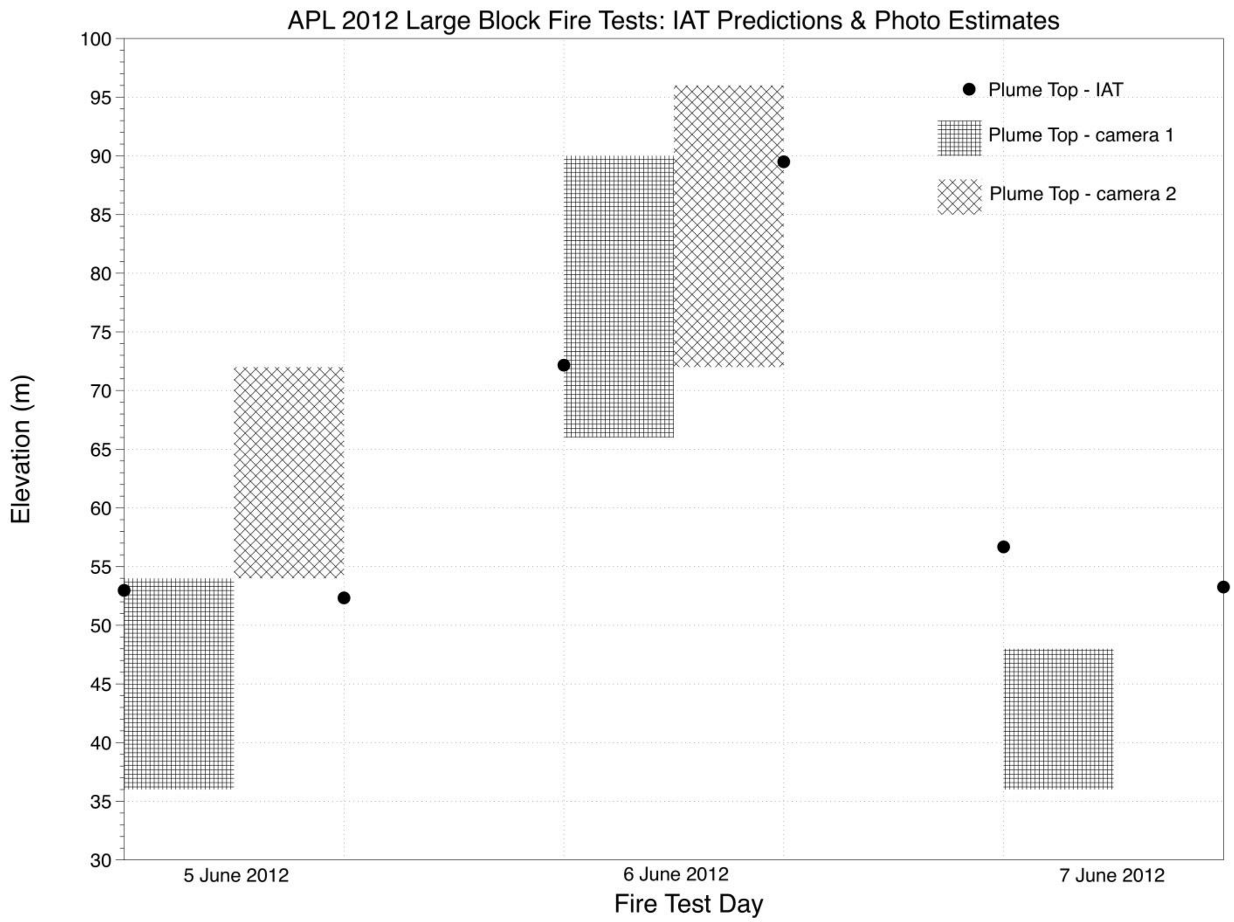

Figure 24: Solid Propellant -- Plume Rise Photogrammetry vs. IAT Simulation

Note the impact of weather on plume trajectory estimates. The two weather files used for each day were at 12:00 noon and 3:00 PM local time for the same day. The figure illustrates the impact weather changes even with this small time difference can have.

As with the earlier Titan 34D data, a significant difference exists in the criteria used to determine plume top. The IAT program assumes material is uniformly distributed through an ideal sphere. The photogrammetric results are based on visual identification of the boundary between the plume and the surrounding atmosphere. This involves estimating the demarcation between plume and ambient as well as "eyeballing" the average of a dynamic topology. As a consequence one would expect some difference in predicted maximum plume elevations. Recall that the photogrammetric results identify plume top.

For June 5, the first test, IAT simulation falls almost exactly on the average of the two photogrammetric estimates. IAT predicts plume top to be between 52.9 and 53.3 meters depending on the weather file used. The average plume top based on photogrammetry is 54 meters with an average standard deviation of 6.4 m. The IAT simulations are well within the uncertainty boundaries of either of the measured plume tops.

The June 6 experiment measured plume tops with an average (81 m) that matches almost exactly the IAT average (80.8 m) for the two weather files used.

On June 7, 2013, camera 2 malfunctioned, leaving only camera 1 for analysis. The estimate of plume top based on this single camera is 42 meters with a 6 m standard deviation. IAT simulations of top of plume elevation for the two weather files are 56.7 m and 53.3 meters for an average of 55.0 meters. This simulation is 2.16 standard deviations above the measured average. However, this measurement had some problems:

1. Camera 2 malfunctioned. The two cameras were used against each other to eliminate interference from clouds in the background. The loss of this ability incurred uncertainty not captured in the published uncertainty estimate.
2. Camera 2 resulted in the higher measurement in the first two tests. If this trend were to have continued, the measured average would have been higher.
3. This puff occurred at a location very close to the ground in a region where NAM data files are extrapolating rather than interpolating.
4. Item three is exacerbated by the fact that at this location, weather data is interpolated from remote known nodes.

Taking the above into account, agreement is reasonable.

Finally plume axial velocities are presented in the following figures. Figure 25 shows a profile of the plume velocities computed using PIV [8]. The axial velocities are order 2 meters/sec above the propellant.

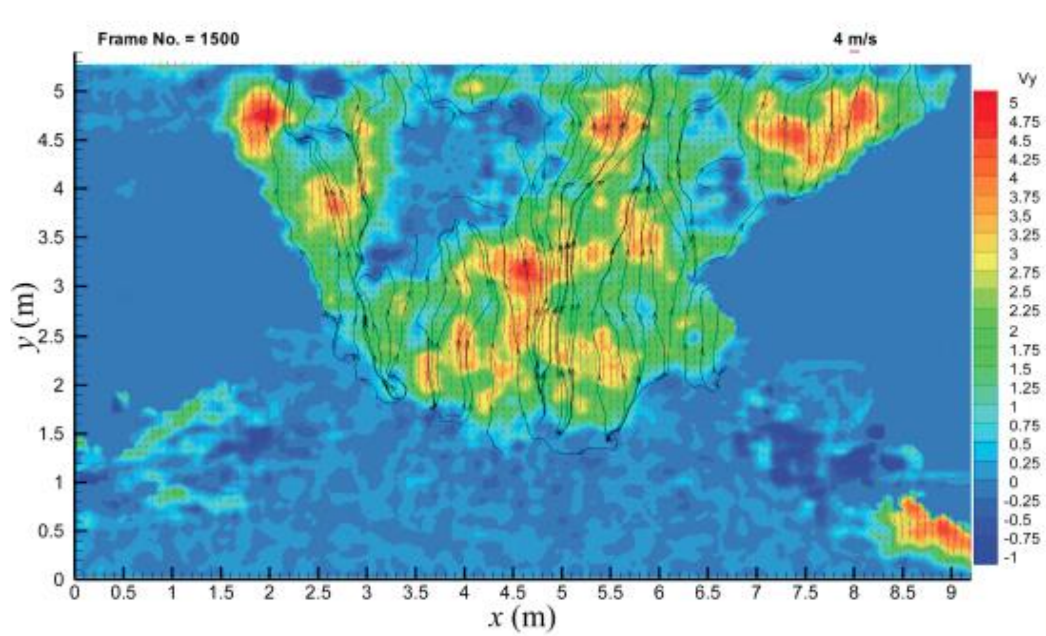

Figure 25: Profile of Plume Velocities [8]

Figure 26 shows an axial velocity profile from IAT where the velocities peak at 2 m/s. This is reasonable comparison.

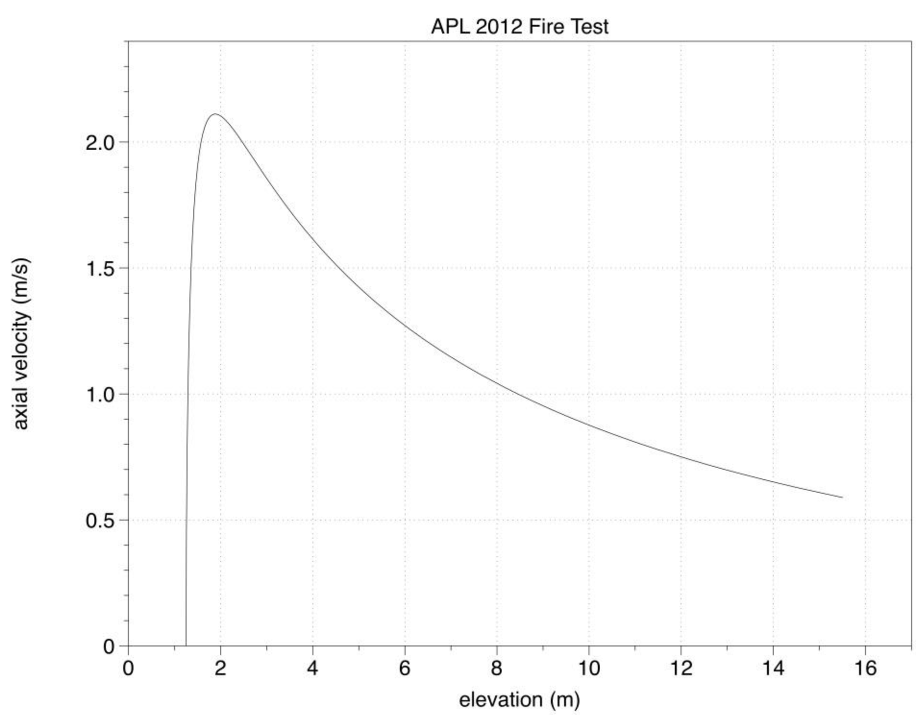

Figure 26: IAT Simulation Axial Velocity

5 Future Work on IAT

As currently written, the IAT works well to predict initial plume height for both liquid fuel fires and solid propellant fires. However, such programs as this can always benefit from improvement. This section describes possible future improvements to the code.

As was pointed out in their respective sections, both the Titan 3D explosion (liquid propellant) and the API test (solid propellant) occurred during neutrally buoyant weather conditions. Since both liquid and solid propellant fires' lofting of radioactive aerosols both contribute significantly to consequence, it would be good to obtain additional validation data for puff rise from both types of burn that occur under turbulent or stable conditions. It is likely this can be done cost effectively in a manner similar to what was done with the 2012 APL tests where plume rise was derived from data taken for other reasons.

Currently, the three entrainment parameters, α_1, α_2 and α_3 are treated as empirical numbers based on experience and published literature. Preliminary examination of α_3 indicates that a relationship exists between it and the TKE parameter already discussed at length in this paper. While no work has been done yet, it would appear feasible that a similar relationship can be developed between α_1 and initial vertical velocity. Consequently, it should be possible to develop and implement algorithms is the code that calculate α_1 and α_3 internally based on initial vertical velocity and TKE respectively.

Future work should address possible material deposition during the puff transport to determine a distribution function for the lofted material. That is the goal is to determine the particle sizes which are entrained in the spherical plume and those in the stem. The axial velocity comparisons presented for both the liquid and solid propellant tests are key to a valid capability to predict the particulate mass distribution function.

6 Summary

The Initial Atmospheric Transport, IAT, computer program is one of the SNL nuclear launch accident consequences analysis computer codes. The purpose of IAT is to predict the initial puff/plume rise resulting from either a solid rocket propellant or liquid rocket fuel fire. The code generates initial conditions for subsequent atmospheric transport calculations.

The Initial Atmosphere Transfer (IAT) code has been compared to two data sets which are appropriate to the design space of space launch accident analyses. The primary model uncertainties are the entrainment coefficients for the extended Taylor model [1, 2, 4]. The Titan 34D accident (1986) was used to calibrate these entrainment settings for a prototypic liquid propellant accident while the recent APL large propellant block tests (2012) were used to calibrate the entrainment settings for prototypic solid propellant accidents. NAM formatted weather data profiles are used by IAT to determine the local buoyancy force balance. The IAT comparisons for the APL solid propellant tests illustrate the sensitivity of the plume elevation to the weather profiles; that is, the weather profile is a dominant factor in determining the plume elevation. <u>For the record, after one minor adjustment to one entrainment parameter, the IAT code performed remarkably well and is considered validated for neutral weather conditions.</u>

Future work should address internal calculation of entrainment parameters, validation under non-neutral weather conditions and distribution of aerosols during the initial rise.

7 References

1. Taylor, Sir Geoffrey 1945, *Dynamics of a mass of hot gas rising in air*, U.S. Atomic Energy Commission MDDC 919. LADC 276.
2. Taylor, Sir Geoffrey, 1950 Proc. Roy. Soc. A, 201, 175.
3. Brown, R. Kolb, C., et. al., *Source Characterization Model (SCM),* SERDP Project CP-1159, ARI-RR-1384, April 2004.
4. Robins, A.G., Apsley, D.D., et. al., *Plume Rise Model Specification,* ADMS 4 P11/020/09.
5. P.J. Linstrom and W.G. mallard, Eds., NIST Chemistry WebBook, NIST Standard Reference database Number 69, June 2005, national Institute of Standards and Technology, Gaithersburg MD, 20899 (http://webbook.nist.gov).
6. Buck, J. Applied Meteorology, Dec. 1981, V20, 1527-1532.
7. Gayle, J.B. and Bransford, J.W., *Size and Duration of Fireballs from Propellant Explosions*, NASA TM X-53314, August 1965.
8. Y.Chang, M.E. White; Solid Rocket Propellant Fire Characterization Test Reports, Volumes I and II; Johns Hopkins Applied Physics Laboratory Report No. TL-13-108 FGX95; June, 2013.
9. Baker, W.E., Cox, P.A., et. al., Explosion Hazards and Evaluation, Elsevier, 1983.
10. Cooper, P.W. and Kurowski, S.R., Intro. to the Technology of Explosives, VCH, 1996.
11. V.J. Dandini; Sandia letter to Earl Wahlquist (DOE); 11/23/1998, SAR Vol. 3, Ref H-1.
12. R.N.Abernathy; Titan 34DF-9 Abort Cloud Measurements – Quantitative Imagery from Two Cameras; Aerospace Corporation; Aerospace Report No. TR-98(1410)-1
13. A. Ponomarenko; RPA: Tool for Rocket Propulsion Analysis Assessment of Delivered Performance of Thrust Chamber; March 2013; http://www.propulsion-analysis.com/downloads/2/docs/RPA_AssessmentOfDeliveredPerformance.pdf
14. M. R. Beychok; Fundamentals of Stack Gas Dispersion, 4th edition; 2005; Self- published.
15. S. Wharton, J Lundquist; *Assessing atmospheric stability and the impacts on wind characteristics at an onshore wind farm. 19th Symposium on Boundary Layers and Turbulent*; Session 2B Observations and Modeling Related to Renewable Energy Application II, 2B.3, 2010.
16. L. S. Lasdon, R. Fox, M. Ratner; *Nonlinear Optimization Using the Generalized Reduced Gradient Method*; Report prepared for the Office of Naval Research, Ad-774 723; 10/1973.F. Gelbard, R.J.Lipinski; Internal Sandia Memo Subject: *Plume Rise from Solid Propellant Fragment Burns at APL in June 2012*; September 3, 2013.

Appendix A. IAT Input Parameters

The following lines are excerpted from the main module of the IAT source code. They provide a cogent description of all the input parameters

```
c
c*****************************************************************************************************************
*************************************
c
c   usage:  iat   puff_init  amb_init value1  value2  value3  value4 value5 value6 value7 value8 ientrain alpha1
                  alpha2 alpha3 vent_min icondense zinitial
c
c*****************************************************************************************************************
*************************************
c
c        if NO comand line inputs, assume inputs from input file:  iat < inputfile
c
c           puff_init  == controls different puff initialization models based on combustion characteristics
c
c                   1 - Liquid propellant
c                     input diamp & tp (default) & RP1 MW distribution (default)
c                     then:
c
c                     value1 == diamp == initial diameter of puff (m)
c                               default = 50 m
c                     value2 == tp    == initial temperature of puff (K)
c                               default = 2700 K
c
c                     NOTE: pressure from atmosphere model assuming puff-atmosphere pressure equilibrium
c
c                   2 - liquid propellant
c                     use databook liquid propellant fire radius-mass relationship to initialize puff
c                     then (english units): diampuff  = 3.769 * masspuff**0.325   !d in (m), m in (Kg)
c                     initial temperature from ideal gas law given Patm, mwt, and density (m/V)
c
c                     value1 == initial mass of RP1  (lb)
c                     value2 == initial mass of LH2  (lb)
c                     value3 == initial mass of Hydrazine (lb)
c
c                     NOTE: pressure from atmosphere model assuming puff-atmosphere pressure equilibrium
c
c                   3 - liquid propellant
c                     use databook liquid propellant radius-mass relationship to initialize puff
c                     then (initial weights SI): diampuff  = 2. * 1.187 * masspuff**0.325   !d in (m), m in (Kg)
c                     initial temperature from ideal gas law given Patm, mwt, and density (m/V)
c
c                     value1 == initial mass of RP1  (kg)
c                     value2 == initial mass of LH2  (kg)
c                     value3 == initial mass of Hydrazine (kg)
c
c                     NOTE: pressure from atmosphere model assuming puff-atmosphere pressure equilibrium
c
c                   4 - solid rocket propellant I
c                     input plume diamp & tp (default) & solid RP MW distribution (internal)
c
c                     value1 == diamp == initial diameter of plume (m)
c                               default = 50 m
c                     value2 == tp    == initial temperature of plume (K)
```

```
c                    default = 2700 K
c
c          NOTE: pressure from atmosphere model assuming puff-atmosphere pressure equilibrium
c
c        5 - solid rocket propellant II
c          input propellant diamp & tp (default) & solid RP MW distribution (internal)
c
c          value1 == diamp == initial diameter of right circle propellant fragment (m)
c                    default = 50 m
c          value2 == tp    == initial temperature of puff (K)
c                    default = 2700 K
c          value3 == area multiplier for initial plume diameter
c                    default = 25
c
c          NOTE: pressure from atmosphere model assuming puff-atmosphere pressure equilibrium
cc
c        6 - solid, above ground, convential explosives (C4, etc)....e.g. Church data
c          use relationship:  initial radius = 0.704 * (E/P)**0.333  (see Boughton...)
c                                   where E = energy release
c                                         P = pressure
c          assume C4 explosive for product of combustion distribution
c
c          value 1 == explosive mass (Kg)
c          value 2 == explosive energy density (MJ/Kg)
c
c          NOTE: pressure from atmosphere model assuming puff-atmosphere pressure equilibrium
c
c        7 - solid, ground level, convential explosives (C4, etc)....e.g. Church data
c          use relationship:  initial radius = 0.856 * (E/P)**0.333  (see Boughton...)
c                                   where E = energy release
c                                         P = pressure
c          assume C4 explosive for product of combustion distribution
c
c          value 1 == explosive mass (Kg)
c          value 2 == explosive energy density (MJ/Kg)
c
c          NOTE: pressure from atmosphere model assuming puff-atmosphere pressure equilibrium
c
c        8 - liquid propellant
c          use an input value of uniform fireball temperature (value8) and ideal gas relationship
c          to get the initial density == diameter
c
c          value1 == initial mass of RP1  (kg)
c          value2 == initial mass of LH2  (kg)
c          value3 == initial mass of Hydrazine (kg)
c          value8 == iniital fireball temperature @ atmosphere pressure (default = 2700K)
c
c          NOTE: pressure from atmosphere model assuming puff-atmosphere pressure equilibrium
c
c        9 - solid rocket propellant -- dense burning zone
c          input propellant total cross-section area, dense burn zone diameter, burn fragment area ratio,
c             tp (default) & solid RP MW distribution (internal)
c
c
c          value1 == initial diameter of dense burning zone (m)
c                    default = 50 m
c          value2 == total cross-section area of all propellant pieces in burn zone (m**2)
c          value3 == area multiplier for initial plume diameter
c                    default = 25
c          value8 == temperature of propellant plume
c
```

```
c                          NOTE: pressure from atmosphere model assuming puff-atmosphere pressure equilibrium
ccc
c
c              amb_init   == controls different ambient atmosphere profile models
c
c                       1 -- use linear temperature lapse profile & exponential pressure profile
c                          then:
c
c                          value4 == dtdz == atmospheric temperature gradieint (K/m or C/m)
c                          value5 == surface temperature (K)
c                          value6 == surface pressure (Pa)
c                          value7 == constant specific relative humidity (gm/kg)
c
c                       2 -- read input file with T, U, V, and P  for nz axial heights, Z (default file = profile.dat)
c
c                             format:       nz
c                             for each z:   z(m)     T(C)    U(m/s)   V(m/s)    p(Pa)  SRH(gm/kg)  TKE(J)
c
c
c                       3 -- read input file from hysplit input (NAM format) (default file = nam.dat)
c
c              ientrain  =  controls the entrainment model options
c
c                      = 1 entrainment Ve = alpha1 * Vbar
c                         vbar = magnitude of 3D relative velocity
c                         threshold velocity for entrainment = vent_min
c
c                      = 2 entrainment Ve = alpha1 * deltaw  (vertical component only)
c                         threshold velocity for entrainment = vent_min
c
c                      = 3 entrainment Ve = alpha1 * deltaw + alpha2 * Vtbar + alpha3*Vturb (default)
c                         Vtbar = magnitude of tranverse velocity (u, v)
c                         Vturb = average turbulent velocity
c                         threshold velocity for entrainment = vent_min
c
c              alpha1 =      entrainment coefficient for Uw (upward velocity)
c                       default = 0.15
c
c              alpha2 =      entrainment coefficient for Uu and Uw (laterial velocity)
c                       default = 0.15
c
c              alpha3 =      entrainment coefficient for turbulent entrainment
c                       default = 0.65
c
c              vent_min  =   minimum velocity for entrainment (m/s)
c                       default = 0.1
c
c              icondense =   controls the condensation model when RH > 1 (relative humidty)
c
c                       = 0 off
c
c                       = 1 on
c                         -condensed water vapor mass forms droplets which
c                          deposit out of the puff
c
c                       = 2 on (default)
c                         -condensed wator vapor forms droplets which remain in
c                          the puff
c
c                zinitial = initial elevation of puff (default = 0.0)
c
```

Appendix B. Weather File Formats

NAM Format 1

```
c          type 1:
c
cMeteorological Profile: 20120605_hysplit.t00z.namsa
c   File start time : 12  6  5  0  0
c   File ending time: 12  6  5 23  0
c
c_______________________________________________________
c Profile Time:  12  6  5 16  0
c Used Nearest Grid Point ( 400, 225) to Lat:    39.62, Lon:   -75.87
c       2D Fields
c       SHGT  MSLP  TPP3  T02M  SOLM  RH2M  U10M  V10M  PRSS  LHTF  SHTF  USTR  RGHS  DSWF
PBLH  TCLD  LCLD  MCLD  HCLD
c          m   hPa    mm    oC          %   m/s   m/s   hPa  W/m2  W/m2  cm/s     m  W/m2     m     %     %     %     %
c  1010  32.0  1012     0  19.5   472  48.4 -0.74  -2.9  1010   252   328  64.6  0.94   952  1976  10.0  10.0     0     0
c       3D Fields
c       TEMP  UWND  VWND  WWND  SPHU  TKEN  PRES    TPOT  UWND  VWND
c         oC   m/s   m/s  mb/h  g/kg  Joul          oK  W->E  S->N
c  1004  17.7 -0.34  -2.2   1.8   6.2   2.2  1007   290.3  -1.2  -1.9
c  1000  17.1 -0.47  -2.6   1.1   6.1   2.5  1003   290.0  -1.5  -2.2
c   995  16.6 -0.53  -2.6   2.3   6.1   2.7   998   290.0  -1.6  -2.2
```

NAM format 2

```
c          type 2:
c
c
c Meteorological Profile: 20120605_nam12
c File start time : 12  6  5  0  0
c File ending time: 12  6  5 21  0
c
c_______________________________________________________
c Profile Time:  12  6  5 12  0
c Used Nearest Grid Point ( 486, 214) to Lat:    39.62, Lon:   -75.87
c       2D Fields
c       SHGT  MSLP  TPP3  CPP3  T02M  RH2M  U10M  V10M  PRSS  LHTF  SHTF  USTR  RGHS  DSWF
c          m   hPa    mm    mm    oC     %   m/s   m/s   hPa  W/m2  W/m2  cm/s     m  W/m2
c  1005  56.1  1012     0     0  13.0  85.7 -0.59  -2.9  1005   136   124  45.0  0.59   440
c       3D Fields
c       UWND  VWND  HGTS  TEMP  WWND  RELH  TKEN    TPOT  UWND  VWND
c        m/s   m/s     m    oC  mb/h     %  Joul      oK  W->E  S->N
c  1000 -0.56  -2.7   100  11.9   2.2  88.7  0.89   285.0  -0.9  -2.6
c   975  -2.8  -4.4   312  10.0   4.5  80.7  0.54   285.2  -3.4  -4.0
c
```

NAM format 3

```
c
c             type 3:
c
c
c Meteorological Profile: 20120605_gdas0p5
c File start time : 12  6  5  0  0
c File ending time: 12  6  5 21  0
c
c___________________________________________________________
c Profile Time:  12  6  5 12  0
c Used Nearest Grid Point ( 569, 260) to Lat:    39.62, Lon:   -75.87
c       2D Fields
c       PRSS  PRT6  UMOF  VMOF  SHTF  DSWF  SH2M  U10M  V10M  T02M  TCLD  SHGT  PBLH  SOLM
LHTF
c        hPa  mm/h            W/m2  W/m2        m/s   m/s    oC     %     m     m       W/m2
c  1010  1010     0  1E-1  0.10 -13.0  56.0  1E-2  -1.8  -2.9  13.1  48.0  33.0   541  0.31  24.0
c       3D Fields
c       TEMP  SPHU  UWND  VWND    TPOT  UWND  VWND
c         oC  g/kg   m/s   m/s      oK  W->E  S->N
c  1009  12.6   8.0  -2.2  -3.5    285.0  -2.2  -3.5
c  1004  12.1   7.7  -2.5  -4.0    284.9  -2.5  -4.0
c
```

User defined format

The user defined atmosphere file, a file called profile.dat, is defined as:

```
c  format:   nz
c           for each z:   z(m)     T(C)    U(m/s)   V(m/s)    p(Pa)  SRH(gm/kg)  TKE(J)
```

B.1 IAT Specific Weather File, Profile.dat for Titan 34D simulation.

This weather data was used for Titan 34D explosion simulations

```
 100     z(m)       T(C)     U(m/s)     V(m/s)      p(Pa) SRH(gm/kg)     TKE(J)
 100.0      16.51      -2.56        3.2   101325.0        4.7        3.5
 125.0      15.98      -2.35        3.3   101000.0       4.55        3.5
 150.0      15.44      -2.15       3.41   100700.0       4.41        3.5
 175.0      14.91      -1.95       3.52   100400.0       4.27        3.5
 200.0      14.37      -1.74       3.62   100100.0       4.14        3.5
 225.0      13.84      -1.54       3.73    99800.0       4.01       1.11
 250.0      14.02      -1.33       3.61    99500.0       4.07       0.66
 275.0      14.48      -1.11       3.41    99200.0        4.2       0.66
 300.0      14.93       -0.9       3.21    98910.0       4.34       0.66
 325.0      15.38      -0.68       3.02    98620.0       4.49       0.66
 350.0      15.83      -0.47       2.82    98330.0       4.64       0.66
 375.0      16.01      -0.29       2.66    98040.0       4.71       0.66
 400.0      15.87      -0.14       2.56    97750.0       4.68       0.99
 425.0      15.73       0.01       2.45    97460.0       4.65       0.99
 450.0      15.59       0.15       2.35    97170.0       4.62       0.99
 475.0      15.45        0.3       2.24    96880.0       4.59       1.04
 500.0      15.28       0.44       2.14    96590.0       4.55       1.32
 525.0       15.0       0.57       2.08    96300.0       4.49       1.57
 550.0      14.73        0.7       2.02    96010.0       4.42       1.57
 575.0      14.45       0.83       1.95    95730.0       4.35       1.57
 600.0      14.18       0.96       1.89    95450.0       4.29       1.57
 625.0       13.9       1.09       1.83    95170.0       4.22       1.17
 650.0       13.8        1.2       1.76    94890.0       4.21       0.85
 675.0      13.72       1.31        1.7    94610.0        4.2       0.82
 700.0      13.64       1.42       1.64    94330.0       4.19       0.82
 725.0      13.56       1.53       1.58    94050.0       4.18       0.82
 750.0      13.48       1.64       1.51    93770.0       4.17       0.82
 775.0       13.4       1.66        1.4    93490.0       4.16       0.82
 800.0      13.32       1.62       1.25    93210.0       4.15       0.82
 825.0      13.24       1.59       1.09    92930.0       4.14       0.82
 850.0      13.16       1.55       0.94    92650.0       4.13       0.82
 875.0      13.08       1.52       0.79    92370.0       4.12       0.91
 900.0      12.93       1.53       0.66    92090.0       4.09       1.25
 925.0      12.66       1.62       0.55    91820.0       4.03       1.54
 950.0      12.39       1.72       0.45    91550.0       3.97       1.57
 975.0      12.11       1.81       0.34    91280.0       3.91       1.57
1000.0      11.84        1.9       0.23    91010.0       3.85       1.54
1025.0      11.57        2.0       0.12    90740.0       3.79       1.54
1050.0       11.3        2.1      -0.02    90470.0       3.74       1.54
1075.0      11.03        2.2      -0.17    90200.0       3.68       1.54
1100.0      10.76        2.3      -0.32    89930.0       3.63       1.54
1125.0      10.49        2.4      -0.47    89660.0       3.57       1.52
1150.0      10.23        2.5      -0.61    89390.0       3.52       1.52
1175.0       9.96       2.64      -0.73    89120.0       3.47       1.52
1200.0        9.7       2.79      -0.85    88850.0       3.42       1.49
1225.0       9.44       2.94      -0.96    88580.0       3.37       1.49
1250.0       9.18       3.09      -1.08    88310.0       3.32       1.49
1275.0       8.92       3.24      -1.19    88040.0       3.27       1.52
1300.0       8.65       3.38      -1.31    87770.0       3.22       1.54
1325.0       8.38       3.51      -1.43    87500.0       3.17       1.54
1350.0       8.11       3.64      -1.55    87230.0       3.12       1.57
1375.0       7.83       3.78      -1.67    86970.0       3.07       1.57
1400.0       7.56       3.91      -1.79    86710.0       3.02       1.54
1425.0       7.29       4.03      -1.91    86450.0       2.98       1.57
1450.0       7.01       4.12       -2.0    86190.0       2.93        1.6
```

1475.0	6.73	4.2	-2.09	85930.0	2.88	1.6
1500.0	6.45	4.29	-2.18	85670.0	2.83	1.6
1525.0	6.17	4.38	-2.27	85410.0	2.79	1.57
1550.0	5.9	4.46	-2.36	85150.0	2.74	1.28
1575.0	5.74	4.43	-2.35	84890.0	2.72	1.07
1600.0	5.57	4.4	-2.35	84630.0	2.7	1.07
1625.0	5.41	4.37	-2.35	84370.0	2.68	1.06
1650.0	5.25	4.34	-2.35	84110.0	2.65	1.06
1675.0	5.09	4.31	-2.35	83850.0	2.63	1.02
1700.0	4.95	4.2	-2.29	83590.0	2.61	0.99
1725.0	4.81	4.06	-2.21	83330.0	2.6	0.99
1750.0	4.67	3.91	-2.12	83070.0	2.58	0.97
1775.0	4.54	3.77	-2.04	82810.0	2.56	0.97
1800.0	4.4	3.63	-1.96	82560.0	2.55	0.99
1825.0	4.26	3.48	-1.88	82310.0	2.53	1.0
1850.0	4.11	3.34	-1.79	82060.0	2.51	1.0
1875.0	3.97	3.19	-1.71	81810.0	2.49	1.0
1900.0	3.82	3.05	-1.62	81560.0	2.47	1.02
1925.0	3.67	2.9	-1.54	81310.0	2.46	1.0
1950.0	3.53	2.76	-1.46	81060.0	2.44	1.0
1975.0	3.38	2.61	-1.37	80810.0	2.42	1.02
2000.0	3.23	2.46	-1.28	80560.0	2.4	1.0
2025.0	3.09	2.31	-1.19	80310.0	2.39	1.0
2050.0	2.94	2.16	-1.1	80060.0	2.37	1.02
2075.0	2.79	2.01	-1.01	79810.0	2.35	0.9
2100.0	2.72	1.86	-0.91	79560.0	2.35	0.79
2125.0	2.66	1.72	-0.82	79310.0	2.34	0.78
2150.0	2.6	1.58	-0.72	79060.0	2.34	0.78
2175.0	2.54	1.44	-0.63	78820.0	2.34	0.78
2200.0	2.48	1.3	-0.53	78580.0	2.33	0.76
2225.0	2.44	1.32	-0.32	78340.0	2.34	0.74
2250.0	2.41	1.44	-0.04	78100.0	2.34	0.73
2275.0	2.38	1.55	0.24	77860.0	2.34	0.73
2300.0	2.35	1.67	0.52	77620.0	2.34	0.73
2325.0	2.32	1.78	0.79	77380.0	2.34	0.7
2350.0	2.33	1.79	1.1	77140.0	2.35	0.66
2375.0	2.43	1.62	1.46	76900.0	2.38	0.66
2400.0	2.52	1.45	1.82	76660.0	2.4	0.66
2425.0	2.62	1.28	2.18	76420.0	2.42	0.66
2450.0	2.71	1.1	2.54	76180.0	2.45	0.66
2475.0	2.8	0.96	2.91	75940.0	2.47	0.66
2500.0	2.88	1.04	3.3	75710.0	2.49	0.66
2525.0	2.95	1.13	3.7	75480.0	2.52	0.66
2550.0	3.03	1.22	4.09	75250.0	2.54	0.66
2575.0	3.11	1.31	4.48	75020.0	2.56	0.66

B.2 NAM Weather Data Files

These files were used to simulate solid rocket propellant test results.

Nam.dat file for June 5, 2012 12:00 Noon

```
Meteorological Profile: 20120605_hysplit.t00z.namsa
 File start time : 12   6   5   0   0
 File ending time: 12   6   5 23   0

___________________________________________________
 Profile Time:   12   6   5 16   0
 Used Nearest Grid Point ( 400, 225) to Lat:    39.62, Lon:   -75.87
        2D Fields
        SHGT  MSLP  TPP3  T02M  SOLM  RH2M  U10M  V10M  PRSS  LHTF  SHTF  USTR  RGHS
DSWF  PBLH  TCLD  LCLD  MCLD  HCLD
           m   hPa    mm    oC           %   m/s   m/s   hPa  W/m2  W/m2  cm/s     m
W/m2     m     %     %     %     %
  1010  32.0  1012     0  19.5   472  48.4 -0.74  -2.9  1010   252   328  64.6  0.94
952  1976  10.0  10.0     0     0
        3D Fields
        TEMP  UWND  VWND  WWND  SPHU  TKEN  PRES     TPOT  UWND  VWND
          oC   m/s   m/s  mb/h  g/kg  Joul             oK  W->E  S->N
  1004  17.7 -0.34  -2.2   1.8   6.2   2.2  1007    290.3  -1.2  -1.9
  1000  17.1 -0.47  -2.6   1.1   6.1   2.5  1003    290.0  -1.5  -2.2
   995  16.6 -0.53  -2.6   2.3   6.1   2.7   998    290.0  -1.6  -2.2
   990  16.1 -0.43  -2.8   2.0   6.1   2.8   993    289.9  -1.5  -2.4
   985  15.7 -0.49  -2.8   3.7   6.1   2.9   988    289.9  -1.6  -2.3
   981  15.1 -0.50  -2.9   3.3   6.0   3.0   983    289.7  -1.6  -2.4
   975  14.7 -0.52  -3.0   2.0   6.0   3.0   978    289.8  -1.7  -2.5
   970  14.2 -0.58  -3.0   2.8   6.0   3.1   972    289.6  -1.7  -2.5
   965  13.8 -0.57  -3.1   3.2   6.0   3.0   967    289.7  -1.8  -2.6
   959  13.2 -0.61  -3.1   4.3   6.0   3.1   962    289.5  -1.8  -2.6
   955  12.7 -0.64  -3.2   3.3   5.9   3.0   956    289.6  -1.9  -2.7
   948  12.2 -0.63  -3.1   3.2   5.9   3.1   949    289.6  -1.8  -2.6
   942  11.6 -0.68  -3.3   3.1   5.8   3.0   944    289.5  -1.9  -2.7
   936  11.0 -0.63  -3.3   3.3   5.9   2.9   937    289.5  -1.9  -2.7
   928  10.4 -0.67  -3.3   4.2   6.0   3.1   929    289.6  -2.0  -2.8
   920   9.7 -0.71  -3.4   4.3   5.9   3.0   922    289.5  -2.0  -2.8
   911   8.9 -0.73  -3.5   4.7   5.9   2.8   914    289.5  -2.1  -2.9
   899   8.0 -0.73  -3.5   4.4   5.9   2.7   904    289.5  -2.1  -2.9
   887   7.0 -0.75  -3.4   4.6   5.8   2.6   892    289.5  -2.1  -2.8
   871   5.8  -1.1  -4.4   6.4   5.8   2.5   879    289.5  -2.8  -3.6
   844   4.0  -1.5  -6.1   9.4   3.8   1.4   847    290.7  -3.8  -5.0
   793   1.3  0.51  -6.4   7.3   3.5     0   806    291.9  -2.1  -6.0
   747  -2.3   2.3  -5.9   2.9   3.0     0   756    293.4  -0.3  -6.3
   685  -4.7  0.82  -6.0     0   1.9     0   699    297.3  -1.7  -5.8
   633  -7.2   3.7  -5.6   2.7   1.1     0   638    302.4   1.1  -6.7
   570 -11.8   7.1  -5.8   3.3   1.0  2E-2   573    306.5   4.2  -8.2
   501 -17.3   9.3  -7.3   4.9  0.51     0   508    310.6   5.6 -10.5
   442 -22.3   7.5  -8.0   5.6  4E-2     0   442    316.8   3.7 -10.4
   377 -29.4   9.2  -8.7   7.0  4E-2     0   378    321.8   4.9 -11.7
   315 -39.1   8.0  -8.6   6.4  1E-1     0   318    324.9   3.9 -11.1
   261 -50.5   9.0  -7.8   4.7  1E-1     0   263    326.2   5.1 -10.8
   217 -53.6   9.7  -3.2   3.9  4E-2     0   218    339.5   7.6  -6.8
   180 -48.3  12.6  -2.5   1.3  2E-3     0   181    366.5  10.5  -7.4
   149 -50.5   9.8  -3.4   1.4  2E-3  2E-2   151    382.3   7.6  -7.1
   121 -54.0   6.4  -3.8 -0.41  2E-3  2E-2   124    398.1   4.4  -6.1
    94 -56.3   2.8  -4.3  -1.1  2E-3  2E-2  98.9    420.2   0.8  -5.0
```

```
   69 -58.6   1.2  -1.5 -0.96  2E-3     0  75.1     449.9   0.5  -1.8
   44 -55.8  -2.1  -2.0 -0.63  2E-3  2E-2  52.3     505.5  -2.7  -1.0
   19 -51.2  -3.2   1.3 -0.15  2E-3  2E-2  29.8     606.1  -2.4   2.4
```

B.3 Nam.dat file for June 5, 2012 3:00 PM

```
Meteorological Profile: 20120605_hysplit.t00z.namsa
 File start time : 12  6  5  0  0
 File ending time: 12  6  5 23  0

__________________________________________________
 Profile Time:  12  6  5 19  0
 Used Nearest Grid Point ( 400, 225) to Lat:    39.62, Lon:   -75.87
        2D Fields
        SHGT  MSLP  TPP3  T02M  SOLM  RH2M  U10M  V10M  PRSS  LHTF  SHTF  USTR  RGHS
DSWF  PBLH  TCLD  LCLD  MCLD  HCLD
           m   hPa    mm    oC           %   m/s   m/s   hPa  W/m2  W/m2  cm/s     m
W/m2     m     %     %     %     %
  1008  32.0  1011     0  20.6   472  45.5 -0.25  -4.0  1008   256   295  67.3  0.94
882  1992  10.0  10.0     0     0
        3D Fields
        TEMP  UWND  VWND  WWND  SPHU  TKEN  PRES      TPOT  UWND  VWND
          oC   m/s   m/s  mb/h  g/kg  Joul              oK  W->E  S->N
  1003  19.0     0  -3.0   1.8   6.3   2.3  1006     291.7  -1.2  -2.7
   998  18.5     0  -3.5   1.4   6.2   2.7  1001     291.5  -1.4  -3.2
   993  17.9     0  -3.7   1.3   6.2   2.8   996     291.4  -1.5  -3.4
   988  17.4     0  -3.9   2.5   6.1   3.1   991     291.3  -1.6  -3.6
   984  17.0     0  -4.0     0   6.2   3.1   986     291.4  -1.6  -3.6
   980  16.5     0  -4.1   2.1   6.1   3.2   981     291.2  -1.6  -3.7
   974  16.1     0  -4.0     0   6.0   3.2   976     291.2  -1.6  -3.7
   969  15.6     0  -4.1     0   6.1   3.3   971     291.2  -1.7  -3.8
   964  15.1 -1E-1  -4.2     0   6.1   3.4   967     291.1  -1.8  -3.8
   958  14.6     0  -4.2     0   6.0   3.3   960     291.2  -1.7  -3.8
   954  14.1 -1E-1  -4.2  -1.5   6.0   3.3   955     291.1  -1.7  -3.8
   947  13.6     0  -4.3     0   6.0   3.3   948     291.2  -1.7  -3.9
   940  13.0     0  -4.3     0   6.0   3.4   943     291.0  -1.7  -4.0
   934  12.4 -0.14  -4.3  -2.5   6.0   3.4   937     290.9  -1.9  -3.9
   927  11.7     0  -4.3  -2.2   5.9   3.4   928     291.1  -1.7  -3.9
   919  11.1     0  -4.3  -2.3   5.9   3.3   922     290.9  -1.7  -4.0
   910  10.3 -0.11  -4.4  -2.4   6.0   3.3   913     290.9  -1.9  -4.0
   898   9.4 -1E-1  -4.4  -1.3   5.9   3.0   903     290.9  -1.9  -4.0
   886   8.4     0  -4.5  -2.3   5.9   2.9   892     290.9  -1.8  -4.1
   869   7.3 -1E-1  -4.5     0   5.9   2.8   879     290.9  -1.9  -4.1
   843   4.2     0  -5.8     0   5.6   2.4   846     290.9  -2.3  -5.3
   792   1.5  0.17  -6.7   7.0   3.9     0   806     292.2  -2.5  -6.2
   747  -1.8   1.6  -5.8  10.5   3.2     0   756     293.9  -0.9  -5.9
   685  -5.7   2.5  -5.3   3.5   2.2     0   699     296.3   0.2  -5.8
   632  -6.8   3.6  -5.8     0  0.73     0   638     302.9   1.0  -6.8
   569 -12.0   6.0  -7.6     0  0.69     0   572     306.4   2.4  -9.3
   500 -15.9   5.3  -7.6     0  0.18     0   507     312.3   1.8  -9.1
   442 -21.8   6.0  -7.8     0  1E-1     0   442     317.5   2.3  -9.5
   377 -29.7   9.9  -6.3     0  1E-1  2E-2   378     321.4   6.5  -9.7
   315 -39.1  12.4  -3.4   4.2  0.11     0   318     325.0  10.0  -8.1
   261 -50.1  14.2  0.21  0.92  1E-1     0   263     326.7  13.1  -5.5
   217 -52.5  12.8   1.8     0  1E-1     0   218     341.1  12.5  -3.5
   180 -49.0  12.2  -1.6   1.2  1E-2     0   181     365.3  10.6  -6.4
   149 -50.2   8.9  -2.3   1.1  2E-3     0   151     382.7   7.2  -5.7
   121 -53.7   6.1  -2.6  0.19  3E-3     0   124     398.8   4.5  -4.9
    94 -56.4   3.3  -1.5  0.61  2E-3  2E-2  98.9     420.0   2.4  -2.7
    69 -58.7   4.4 -0.58  0.11  2E-3  2E-2  75.1     449.7   3.8  -2.3
    44 -57.0  -1.1  -2.5  1E-1  2E-3  2E-2  52.3     502.8  -2.0  -1.8
    19 -52.3  -5.4 -0.56  0.35  2E-3  2E-2  29.8     603.1  -5.2   1.7
```

B.4 Nam.dat file for June 6, 2012 12:00 Noon

```
 Meteorological Profile: 20120605_hysplit.t00z.namsa
 File start time : 12  6  5  0  0
 File ending time: 12  6  5 23  0

___________________________________________________
 Profile Time:   12  6  5 16  0
 Used Nearest Grid Point ( 400, 225) to Lat:    39.62, Lon:   -75.87
        2D Fields
        SHGT  MSLP  TPP3  T02M  SOLM  RH2M  U10M  V10M  PRSS  LHTF  SHTF  USTR
RGHS  DSWF  PBLH  TCLD  LCLD  MCLD  HCLD
           m   hPa    mm    oC           %   m/s   m/s   hPa  W/m2  W/m2  cm/s
m  W/m2     m     %     %     %     %
  1010  32.0  1012     0  19.5   472  48.4 -0.74  -2.9  1010   252   328  64.6
0.94   952  1976  10.0  10.0     0     0
        3D Fields
        TEMP  UWND  VWND  WWND  SPHU  TKEN  PRES     TPOT  UWND  VWND
          oC   m/s   m/s  mb/h  g/kg  Joul            oK  W->E  S->N
  1004  17.7 -0.34  -2.2   1.8   6.2   2.2  1007    290.3  -1.2  -1.9
  1000  17.1 -0.47  -2.6   1.1   6.1   2.5  1003    290.0  -1.5  -2.2
   995  16.6 -0.53  -2.6   2.3   6.1   2.7   998    290.0  -1.6  -2.2
   990  16.1 -0.43  -2.8   2.0   6.1   2.8   993    289.9  -1.5  -2.4
   985  15.7 -0.49  -2.8   3.7   6.1   2.9   988    289.9  -1.6  -2.3
   981  15.1 -0.50  -2.9   3.3   6.0   3.0   983    289.7  -1.6  -2.4
   975  14.7 -0.52  -3.0   2.0   6.0   3.0   978    289.8  -1.7  -2.5
   970  14.2 -0.58  -3.0   2.8   6.0   3.1   972    289.6  -1.7  -2.5
   965  13.8 -0.57  -3.1   3.2   6.0   3.0   967    289.7  -1.8  -2.6
   959  13.2 -0.61  -3.1   4.3   6.0   3.1   962    289.5  -1.8  -2.6
   955  12.7 -0.64  -3.2   3.3   5.9   3.0   956    289.6  -1.9  -2.7
   948  12.2 -0.63  -3.1   3.2   5.9   3.1   949    289.6  -1.8  -2.6
   942  11.6 -0.68  -3.3   3.1   5.8   3.0   944    289.5  -1.9  -2.7
   936  11.0 -0.63  -3.3   3.3   5.9   2.9   937    289.5  -1.9  -2.7
   928  10.4 -0.67  -3.3   4.2   6.0   3.1   929    289.6  -2.0  -2.8
   920   9.7 -0.71  -3.4   4.3   5.9   3.0   922    289.5  -2.0  -2.8
   911   8.9 -0.73  -3.5   4.7   5.9   2.8   914    289.5  -2.1  -2.9
   899   8.0 -0.73  -3.5   4.4   5.9   2.7   904    289.5  -2.1  -2.9
   887   7.0 -0.75  -3.4   4.6   5.8   2.6   892    289.5  -2.1  -2.8
   871   5.8  -1.1  -4.4   6.4   5.8   2.5   879    289.5  -2.8  -3.6
   844   4.0  -1.5  -6.1   9.4   3.8   1.4   847    290.7  -3.8  -5.0
   793   1.3  0.51  -6.4   7.3   3.5     0   806    291.9  -2.1  -6.0
   747  -2.3   2.3  -5.9   2.9   3.0     0   756    293.4  -0.3  -6.3
   685  -4.7  0.82  -6.0     0   1.9     0   699    297.3  -1.7  -5.8
   633  -7.2   3.7  -5.6   2.7   1.1     0   638    302.4   1.1  -6.7
   570 -11.8   7.1  -5.8   3.3   1.0  2E-2   573    306.5   4.2  -8.2
   501 -17.3   9.3  -7.3   4.9  0.51     0   508    310.6   5.6 -10.5
   442 -22.3   7.5  -8.0   5.6  4E-2     0   442    316.8   3.7 -10.4
   377 -29.4   9.2  -8.7   7.0  4E-2     0   378    321.8   4.9 -11.7
   315 -39.1   8.0  -8.6   6.4  1E-1     0   318    324.9   3.9 -11.1
   261 -50.5   9.0  -7.8   4.7  1E-1     0   263    326.2   5.1 -10.8
   217 -53.6   9.7  -3.2   3.9  4E-2     0   218    339.5   7.6  -6.8
   180 -48.3  12.6  -2.5   1.3  2E-3     0   181    366.5  10.5  -7.4
   149 -50.5   9.8  -3.4   1.4  2E-3  2E-2   151    382.3   7.6  -7.1
   121 -54.0   6.4  -3.8 -0.41  2E-3  2E-2   124    398.1   4.4  -6.1
    94 -56.3   2.8  -4.3  -1.1  2E-3  2E-2  98.9    420.2   0.8  -5.0
    69 -58.6   1.2  -1.5 -0.96  2E-3     0  75.1    449.9   0.5  -1.8
    44 -55.8  -2.1  -2.0 -0.63  2E-3  2E-2  52.3    505.5  -2.7  -1.0
    19 -51.2  -3.2   1.3 -0.15  2E-3  2E-2  29.8    606.1  -2.4   2.4
```

B.5 Nam.dat file for June 6, 2012 3:00 PM

```
 Meteorological Profile: 20120606_hysplit.t00z.namsa
 File start time : 12  6  6  0  0
 File ending time: 12  6  6 23  0

___________________________________________________
 Profile Time:  12  6  6 19  0
 Used Nearest Grid Point ( 400, 225) to Lat:    39.62, Lon:   -75.87
        2D Fields
        SHGT  MSLP  TPP3  T02M  SOLM  RH2M  U10M  V10M  PRSS  LHTF  SHTF  USTR
RGHS  DSWF  PBLH  TCLD  LCLD  MCLD  HCLD
           m   hPa    mm    oC           %   m/s   m/s   hPa  W/m2  W/m2  cm/s
m  W/m2     m     %     %     %     %
  1013  32.0  1015  0.24  21.8   472  50.1  1E-1  0.14  1013   248   125  43.3
0.94   431  1982  91.0  69.0  69.0     0
        3D Fields
        TEMP  UWND  VWND  WWND  SPHU  TKEN  PRES      TPOT  UWND  VWND
          oC   m/s   m/s  mb/h  g/kg  Joul              oK  W->E  S->N
  1007  20.7  0.47  1E-1     0   7.4   1.1  1011     293.0   0.5  -0.1
  1002  20.2  0.55  0.16     0   7.3   1.5  1006     292.8   0.6  -0.1
   997  19.6  0.56  0.13   1.8   7.2   1.6  1001     292.7   0.6  -0.1
   992  19.3  0.64  0.22  -1.1   7.2   1.8   996     292.8   0.7  -0.1
   988  18.8  0.61  0.18     0   7.2   1.8   991     292.7   0.6  -0.1
   984  18.3  0.58  0.22     0   7.2   2.0   986     292.7   0.6   0.0
   978  17.9  0.60  0.22   1.8   7.1   2.0   981     292.6   0.6   0.0
   973  17.4  0.70  0.14     0   7.1   2.0   976     292.6   0.7  -0.2
   968  16.9  0.69  0.15     0   7.1   2.1   970     292.7   0.7  -0.1
   962  16.5  0.73  0.19     0   7.1   2.1   964     292.7   0.7  -0.1
   957  16.0  0.71  0.17     0   7.1   2.2   958     292.7   0.7  -0.1
   950  15.5  0.73  0.19     0   7.1   2.1   953     292.7   0.7  -0.1
   944  14.8  0.74  0.17   1.1   7.1   2.3   946     292.6   0.7  -0.1
   938  14.2  0.84  0.19     0   7.0   2.1   939     292.6   0.8  -0.2
   931  13.6  0.85  0.11     0   7.1   2.0   932     292.5   0.8  -0.2
   923  13.0  0.82  0.15     0   7.0   2.0   924     292.6   0.8  -0.2
   914  12.2  0.86  0.22     0   7.0   2.1   916     292.6   0.9  -0.1
   901  11.3  0.83  0.22     0   7.0   2.1   906     292.6   0.9  -0.1
   889  10.2  0.86  0.12     0   7.0   2.0   894     292.6   0.8  -0.2
   873   9.0  0.99  1E-1     0   6.9   2.0   882     292.5   0.9  -0.3
   846   6.2   2.0  -1.3   1.8   5.7   1.1   849     292.8   1.3  -2.0
   795   3.9   2.1  -1.2   3.5   4.9     0   808     294.4   1.4  -2.0
   749  0.48   1.7 -0.69   3.5   4.0     0   758     296.2   1.3  -1.3
   687  -3.3   1.2  -1.0   3.5   3.2     0   701     298.7   0.7  -1.4
   634  -7.0  0.39  -1.9  -1.9   2.8     0   638     302.6  -0.4  -1.9
   570 -12.8  0.20  -1.4  -3.5   1.7     0   573     305.3  -0.4  -1.4
   501 -18.9   3.6 -0.50  -3.7  0.74     0   508     308.6   3.1  -1.9
   442 -24.7   8.4  0.35  -6.1  1E-1     0   443     313.7   7.9  -3.1
   377 -32.3  11.2   1.9  -4.6  0.16     0   379     318.0  11.0  -2.7
   315 -42.2  14.0   3.7  -2.6  1E-1     0   318     320.7  14.3  -2.3
   261 -51.6  15.4   7.8     0  1E-1     0   263     324.6  17.3   0.9
   217 -47.6  18.6   8.0  -2.4  3E-2     0   218     348.6  20.2  -0.2
   180 -48.1  15.9   4.6  -1.1  2E-2     0   181     366.8  16.4  -2.2
   149 -52.2  13.3   6.3     0  1E-2     0   151     379.4  14.7   0.4
   121 -54.0  12.4   6.3   1.2  1E-2     0   124     398.1  13.9   0.8
    94 -56.5  10.3   3.1  0.53  3E-3  2E-2  98.9     419.9  10.6  -1.3
    69 -57.7   5.3   1.1 -0.85  2E-3  2E-2  75.1     451.8   5.3  -1.1
    44 -55.5   1.5   3.8 -0.87  2E-3  2E-2  52.3     506.3   2.9   2.9
    19 -53.0  -3.6 -0.62 -0.65  2E-3  2E-2  29.8     601.3  -3.5   0.9
```

B.6 Nam.dat file for June 7, 2012 12:00 Noon

```
 Meteorological Profile: 20120607_hysplit.t00z.namsa
 File start time : 12   6   7   0   0
 File ending time: 12   6   7 23   0

____________________________________________________
 Profile Time:  12   6   7 16   0
 Used Nearest Grid Point ( 400, 225) to Lat:    39.62, Lon:   -75.87
        2D Fields
        SHGT  MSLP  TPP3  T02M  SOLM  RH2M  U10M  V10M  PRSS  LHTF  SHTF  USTR  RGHS
DSWF  PBLH  TCLD  LCLD  MCLD  HCLD
           m   hPa    mm    oC           %   m/s   m/s   hPa  W/m2  W/m2  cm/s     m
W/m2     m     %     %     %     %
  1011  32.0  1016     0  25.1   464  45.6   3.1     0  1011   288   271  62.1  0.94
940  2013  10.0  10.0     0     0
        3D Fields
        TEMP  UWND  VWND  WWND  SPHU  TKEN  PRES     TPOT  UWND  VWND
          oC   m/s   m/s  mb/h  g/kg  Joul             oK  W->E  S->N
  1005  23.3   2.5     0  0.88   8.3   1.8  1011    295.6   2.3  -1.0
  1001  22.9   2.8 -1E-1   1.8   8.1   2.4  1006    295.5   2.5  -1.2
   996  22.3   3.0     0  0.88   8.1   2.6  1001    295.4   2.7  -1.2
   991  21.9   3.0     0   1.2   8.1   2.8   996    295.4   2.8  -1.2
   987  21.3   3.1     0     0   8.0   2.9   990    295.3   2.8  -1.2
   983  20.9   3.2     0     0   8.0   3.0   986    295.3   2.9  -1.3
   976  20.4   3.1     0  0.88   8.0   3.0   981    295.2   2.9  -1.3
   971  20.0   3.3     0   1.2   7.9   3.0   976    295.2   3.0  -1.3
   966  19.4   3.3     0     0   7.9   3.1   971    295.0   3.0  -1.3
   960  18.9   3.2 -1E-1     0   7.9   3.1   964    295.2   2.9  -1.4
   956  18.4   3.3     0     0   7.9   3.2   959    295.0   3.0  -1.3
   949  17.9   3.3     0  -2.1   7.9   3.2   953    295.1   3.0  -1.3
   943  17.3   3.4 -1E-1  -2.7   7.9   3.2   945    295.2   3.1  -1.5
   937  16.7   3.4 -0.11  -2.3   7.8   3.1   939    295.2   3.0  -1.5
   930  16.0   3.5     0  -2.0   7.9   3.1   933    295.0   3.2  -1.4
   921  15.3   3.5 -0.14  -2.6   7.8   3.1   924    295.1   3.1  -1.5
   912  14.6   3.6 -0.10  -2.4   7.8   2.9   915    295.1   3.2  -1.5
   900  13.6   3.6     0  -4.7   7.8   2.9   905    295.1   3.3  -1.4
   888  12.6   3.5 -0.11  -4.4   7.8   2.8   894    295.2   3.2  -1.5
   871  11.4   3.6     0  -4.6   7.7   2.8   882    294.9   3.3  -1.5
   845   8.7   5.0 -0.25  -6.3   6.1   2.3   849    295.3   4.5  -2.3
   794   5.5   5.8  0.48  -7.0   5.1     0   809    296.1   5.5  -1.9
   748   1.8   4.5 -0.20  -1.3   4.2     0   758    297.6   4.0  -2.0
   686  -3.0   4.9 -0.45   2.2   3.1     0   701    299.1   4.3  -2.4
   633  -5.9   6.5  0.26   2.5   2.3  2E-2   639    303.8   6.0  -2.4
   570 -10.8  10.0 -0.48   5.3   1.8     0   574    307.4   8.9  -4.5
   501 -17.4  11.0  -2.4   7.5  0.91     0   508    310.5   9.1  -6.6
   442 -25.3   9.6  -3.3   5.2  0.35  2E-2   442    313.0   7.5  -6.9
   377 -34.2   6.6  -1.9   3.8  0.13  2E-2   379    315.5   5.3  -4.4
   315 -44.2   7.6 -0.76  -1.8  1E-1     0   318    317.9   6.7  -3.8
   261 -51.4  13.3     0  -3.5  4E-2     0   263    324.8  12.2  -5.4
   217 -48.2  21.2   4.5  -2.6  3E-2  2E-2   218    347.7  21.2  -4.4
   180 -49.0  24.2   3.5  0.60  3E-2     0   181    365.3  23.5  -6.6
   149 -53.0  23.1   1.6  0.55  1E-2     0   151    377.9  21.8  -7.8
   121 -55.6  20.7   1.5   1.1  1E-2  2E-2   124    395.3  19.6  -6.9
    94 -57.7  15.6 -1E-1   1.6  2E-3     0  98.9    417.5  14.3  -6.4
    69 -58.1   8.6   1.1   1.2  2E-3  2E-2  75.1    451.0   8.3  -2.5
    44 -55.2  0.95 -0.18  0.30  2E-3  2E-2  52.3    507.0   0.8  -0.6
    19 -51.8  -4.1  0.75  0.81  2E-3  2E-2  29.8    604.4  -3.4   2.3
```

B.7 Nam.dat file for June 7, 2012 12:00 Noon

```
 Meteorological Profile: 20120607_hysplit.t00z.namsa
 File start time : 12   6   7  0   0
 File ending time: 12   6   7 23   0

____________________________________________________
 Profile Time:   12   6   7 19   0
 Used Nearest Grid Point ( 400, 225) to Lat:     39.62, Lon:    -75.87
        2D Fields
        SHGT  MSLP  TPP3  T02M  SOLM  RH2M  U10M  V10M  PRSS  LHTF  SHTF  USTR
RGHS  DSWF  PBLH  TCLD  LCLD  MCLD  HCLD
           m   hPa    mm    oC           %   m/s   m/s   hPa  W/m2  W/m2  cm/s
m  W/m2     m     %     %     %     %
  1011  32.0  1013     0  25.6   464  45.6   3.1  -1.2  1011   280   245  64.4
0.94   866  2557  10.0  10.0     0     0
        3D Fields
        TEMP  UWND  VWND  WWND  SPHU  TKEN  PRES     TPOT  UWND  VWND
          oC   m/s   m/s  mb/h  g/kg  Joul            oK  W->E  S->N
  1005  24.1   2.7  -1.1   3.1   8.5   2.1  1008     296.6   2.0  -2.1
  1000  23.4   3.1  -1.1   2.7   8.3   2.5  1004     296.2   2.4  -2.3
   995  22.9   3.3  -1.1   1.5   8.4   2.7   999     296.2   2.5  -2.4
   990  22.5   3.3  -1.2   2.6   8.4   3.0   994     296.1   2.5  -2.5
   986  22.1   3.5  -1.2     0   8.3   3.0   989     296.1   2.7  -2.5
   982  21.6   3.4  -1.2     0   8.3   3.1   984     296.1   2.6  -2.5
   976  21.0   3.5  -1.2  -1.1   8.3   3.1   979     296.0   2.8  -2.5
   971  20.6   3.5  -1.2  -1.4   8.2   3.2   973     296.0   2.7  -2.5
   966  20.1   3.5  -1.2  -2.0   8.2   3.2   968     296.0   2.7  -2.5
   960  19.6   3.6  -1.2  -1.8   8.2   3.3   962     296.0   2.8  -2.6
   956  19.1   3.6  -1.2  -2.6   8.2   3.3   956     296.0   2.8  -2.6
   948  18.6   3.6  -1.2  -3.2   8.2   3.3   951     296.0   2.9  -2.6
   942  17.9   3.7  -1.2  -3.1   8.1   3.3   944     295.9   2.9  -2.6
   936  17.4   3.6  -1.2  -3.5   8.2   3.3   937     296.0   2.8  -2.6
   929  16.7   3.8  -1.2  -5.3   8.1   3.3   931     295.8   3.0  -2.6
   921  16.0   3.8  -1.2  -5.3   8.2   3.3   922     295.9   3.0  -2.6
   912  15.2   3.8  -1.1  -7.0   8.2   3.1   914     295.9   3.0  -2.5
   900  14.3   3.8  -1.1  -6.0   8.1   3.1   904     295.9   3.1  -2.6
   887  13.3   3.8  -1.2  -7.1   8.1   3.0   892     295.9   3.0  -2.6
   871  12.0   3.8  -1.1  -9.4   8.1   2.9   879     295.9   3.0  -2.5
   844   9.0   3.9  -1.2 -10.6   8.0   2.5   847     295.9   3.1  -2.7
   794   6.0   7.9  -1.6 -12.2   6.2     0   806     296.8   6.6  -4.6
   748   1.9   6.7  -1.9  -5.6   4.8     0   757     297.9   5.4  -4.5
   686  -3.1   6.7  -1.5   3.5   2.8     0   700     299.1   5.6  -4.1
   633  -6.7   6.7  -1.8   6.5   1.7     0   637     303.1   5.5  -4.3
   570 -11.1   9.1  -2.0   1.5  0.53     0   573     307.3   7.5  -5.5
   501 -16.5  10.9  -2.1     0  0.22     0   508     311.5   9.2  -6.3
   442 -25.0  11.0 -0.22   3.5  0.18     0   442     313.3   9.9  -4.6
   377 -34.0   7.8   2.3   5.3  0.15  2E-2   378     315.8   8.1  -1.0
   315 -44.2   9.2   2.2   7.9  1E-1  2E-2   318     317.9   9.3  -1.7
   261 -50.6  17.0   2.2     0  3E-2     0   263     326.0  16.4  -4.8
   217 -47.3  25.8   3.8     0  3E-2     0   218     349.2  25.2  -6.9
   180 -48.4  23.3   1.6   3.5  3E-2     0   181     366.3  21.9  -8.0
   149 -53.1  22.7   1.5   3.2  1E-2     0   151     377.9  21.4  -7.8
   121 -56.0  21.0   1.4   2.3  4E-3  2E-2   124     394.6  19.8  -7.1
    94 -57.1  14.5  0.65   1.2  2E-3  2E-2  98.9     418.8  13.5  -5.2
    69 -57.8  11.0   2.6     0  2E-3  2E-2  75.1     451.5  11.1  -2.0
    44 -55.2   3.7  0.47 -0.71  2E-3  2E-2  52.3     506.9   3.6  -1.1
    19 -52.4  -2.2 -0.63 -0.47  2E-3  2E-2  29.8     602.7  -2.2   0.3
```

Appendix C. Gelbard/Lipinski Memo

Sandia National Laboratories
Operated for the U.S. Department of Energy by
Sandia Corporation

Albuquerque, New Mexico 87185-

date: September 3, 2013

to: T. J. Bartel, Org 6223, MS-0747

from: F. Gelbard and R. J. Lipinski, Org 6223, MS-0747

subject: Plume Rise from Solid Propellant Fragment Burns at APL in June 2012

The Johns Hopkins University Applied Physics Laboratory (JHU/APL, or simply APL) performed some open-air burns of solid propellant at the Alliant Technology (ATK) burn site in Elkton, MD in June of 2013. The plumes from these burns were photographed via digital video cameras. Table 13 shows the characteristics of the propellant fragments used in these burns. All three were right circular cylinders. In all three cases, the burning occurred on the bottom surface and the side surfaces. The burns occurred on a raised platform about 1 m above the ground and 8 ft (2.4 m) in diameter.

Table 13. Characteristics of the three propellant burn fragments.

Date	Diameter	Height	Substrate
5 June 2012	20 in (0.508 m)	10 in (0.254 m)	FlexFram on Steel
6 June 2012	20 in (0.508 m)	10 in (0.254 m)	KSC Concrete
7 June 2012	20 in (0.508 m)	10 in (0.254 m)	KSC Concrete

Figure 27 shows an aerial view of the burn site along with the location of the two video cameras. A row of trees lines the creek bank in the background. These provide a convenient scale for plume height in the videos, once parallax is accounted for. Figure 28 shows a close-up of the test area, including a 26-ft (7.9-m) tall scaffold. Figure 29 shows photo of the scaffold used to hold a laser target; the yellow tape markers on the scaffold are at 5-ft (1.52 m) intervals. The scaffold can be used for calibration in the videos of the plume. The trees in the background are also a potential tool for calibration, but they are of varying height and different distances from the plume; the scaffold is less confusing option.

Figure 30 shows a frame from the start of the video for the burn on June 5, 2012. The 25-ft section of the scaffold (from the base to just below the top of the white laser target) extends vertically for 38 pixels for camera #2 (left) and 42 pixels for camera #1 (right). Inspection of the videos for the three burns shows that this calibration is valid for all three days.

Figure 27. Aerial view of burn site and camera locations (Google Earth). North is up.

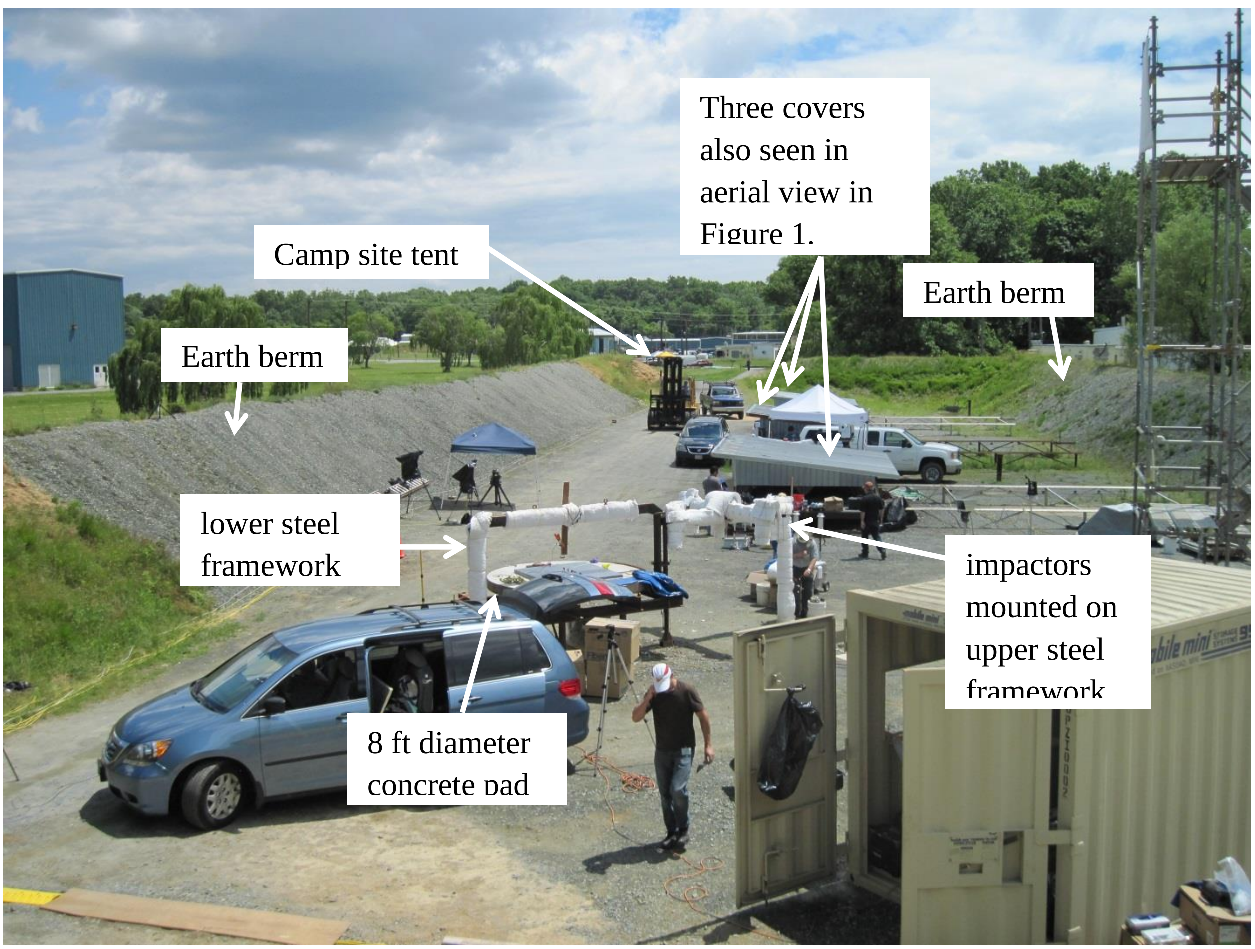

Figure 28. Experimental arrangement at burn site, looking south. The scaffold is on the right.

Figure 29. Close-up of the 26-ft (7.9-m) tall scaffold and creek bank trees.

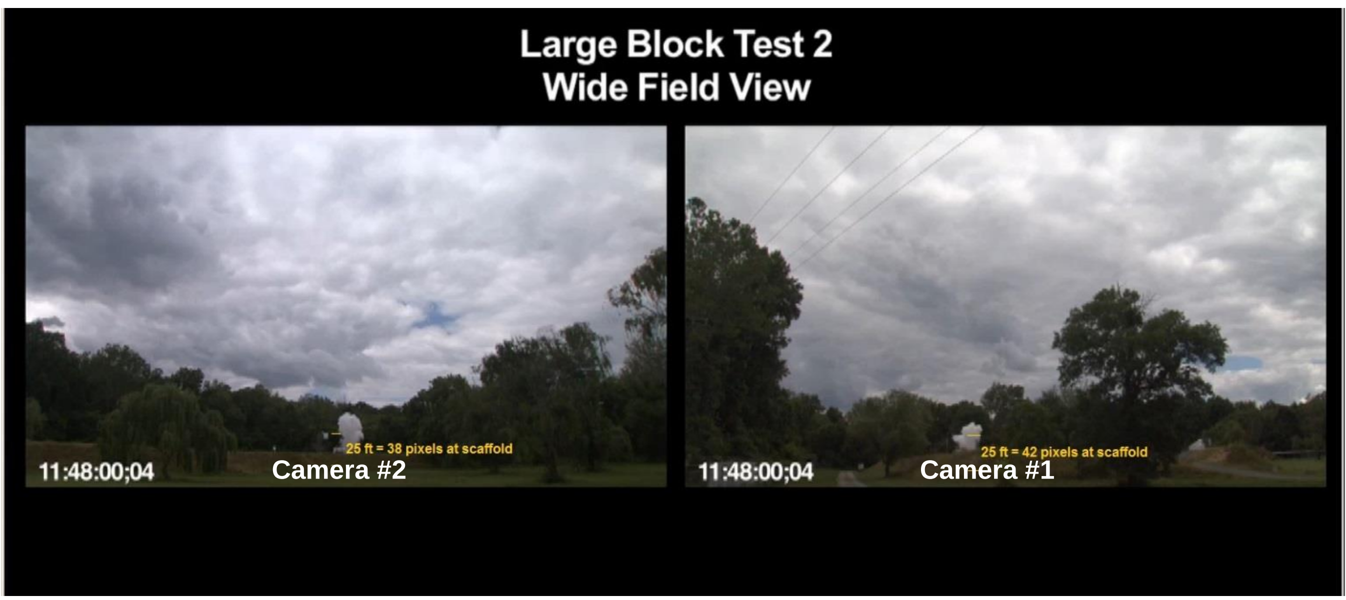

Figure 30. Video camera frames at start of burn on June 5, 2012.

June 5, 2012 Burn

Inspection of the videos show that the plume takes about 60 sec to reach its full height and then start to move sideways in the wind. On day 1 there was a considerable wind that knocked down the plume from time to time. The image for day 1 was chosen to be right after such an event. The faint plume that was knocked down can be seen just to the left of the denser plume in the view from Camera 2 in Figure 31.

An estimate of the plume footprint was made for each burn based on the views from each camera and whether the plume was in front of or behind key trees and other landmarks. These footprints are shown in an aerial view for each burn. These plume plots are used to establish the correct parallax correction factor for each burn and each camera. Figure 32 shows such a view for the burn on June 5, 2012. The white scalloped outline is an estimate of where the plume was at 1 min, 11 sec into the burn. The fainter portion of the sketch represents the fainter portion of the plume (in Figure 31) that had been knocked down by the wind.

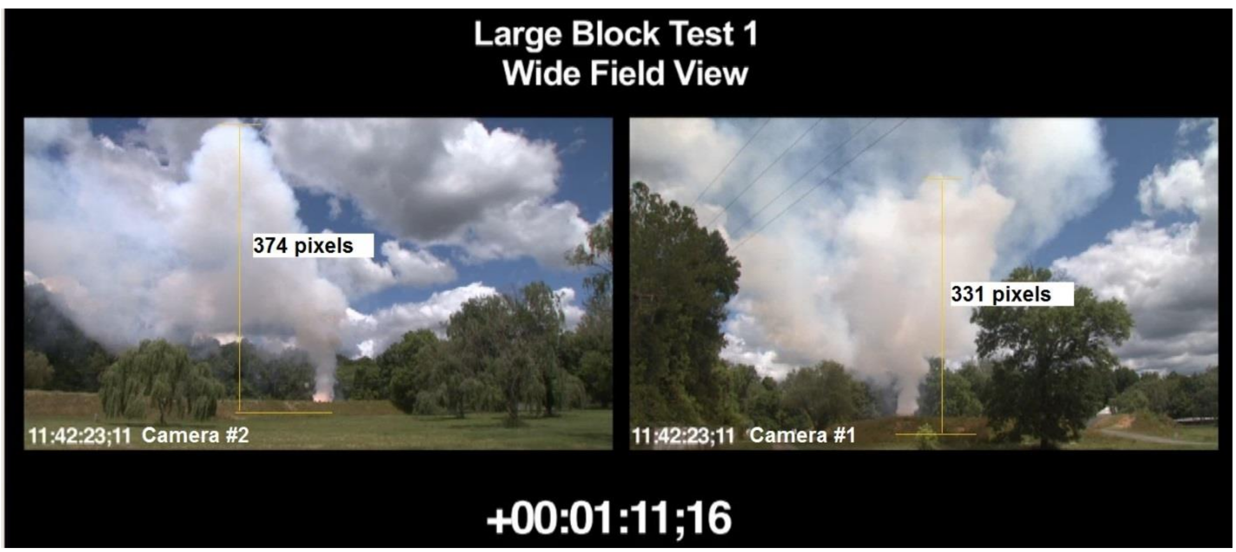

Figure 31. Video camera frames at 1 min 11 sec into the burn on June 5, 2012.

Figure 32. Arial view of estimated plume extent at 1 min 11 sec into the burn on June 5, 2012.

The orange X in Figure 32 marks the spot where the plume height is estimated. It corresponds to the orange horizontal lines in Figure 31. The distance from camera #1 to the top of the plume divided by the distance from camera #1 to the scaffold is 0.73. (The scaffold is west of the red dot in the figure.) Hence, the height of the plume, as determined by camera #1, is ((25 ft)/(42 pixels)) x (331 pixels) x (0.74 for parallax) = 146 ft. For camera #2 the ratio is 0.88, and the plume height is ((25 ft)/(38 pixels) x (374 pixels) x (0.84 for parallax) = 207 ft. The uncertainty is about 15%, or about 30 ft.

June 6, 2012 Burn

Figure 33 and Figure 34 show similar figures for the burn on June 6, 2012. The estimated plume height from camera #1 is ((25 ft)/(42 pixels)) x (321 pixels) x (1.34 for parallax) = 256 ft. For camera #2 it is ((25 ft)/(42 pixels)) x (384 pixels) x (1.21 for parallax) = 276 ft. The uncertainty is about 15%, or about 40 ft.

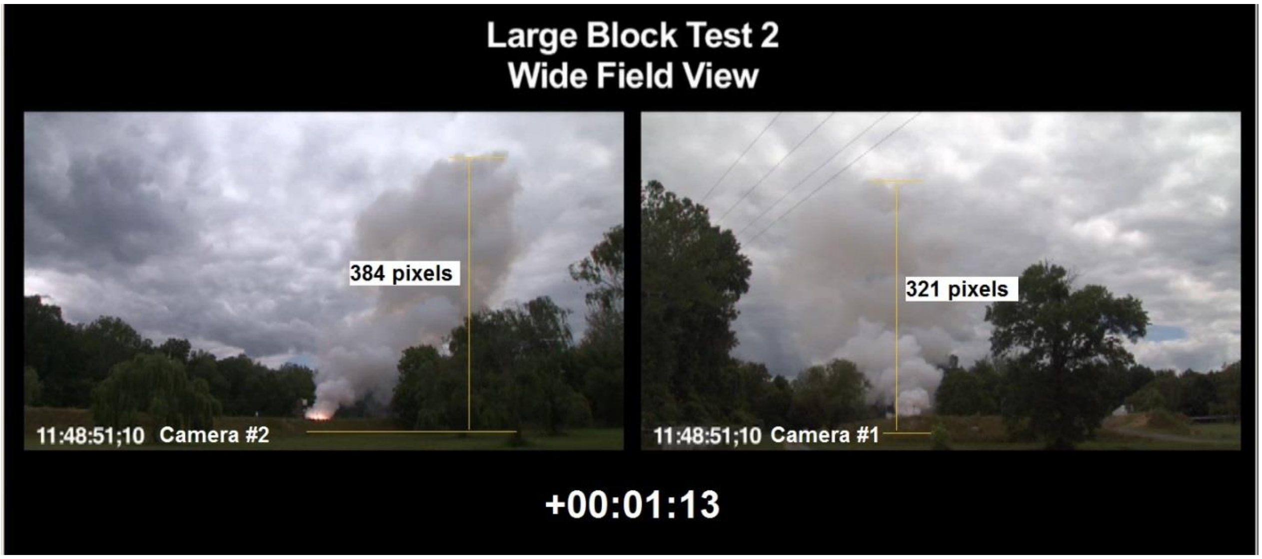

Figure 33. Video camera frames at 1 min 13 sec into the burn on June 6, 2012.

Figure 34. Arial view of estimated plume extent at 1 min 13 sec into the burn on June 6, 2012.

Burn 3: June 7, 2012

Figure 35 and Figure 36 show similar figures for the burn on June 7, 2012. The estimated plume height from camera #1 is ((25 ft)/(42 pixels)) x (415 pixels) x (0.56 for parallax) = 138 ft. The uncertainty is about 15%, or about 20 ft.

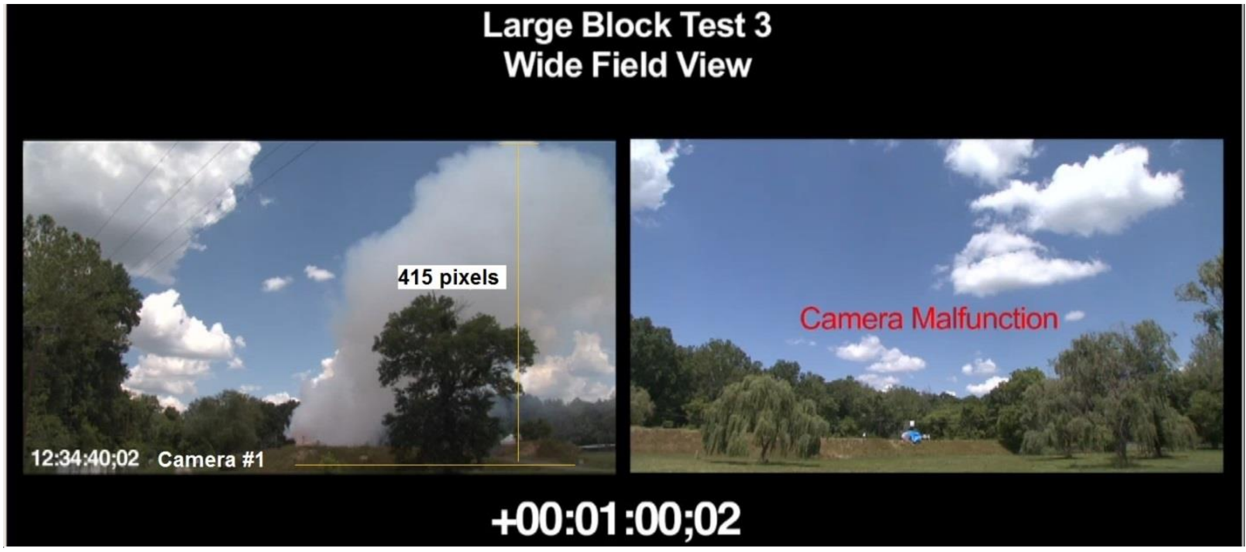

Figure 35. Video camera frames at 0 min 59 sec into the burn on June 7, 2012.

Figure 36. Arial view of estimated plume extent at 0 min 59 sec into the burn on June 7, 2012.

Summary

A summary of estimated plume heights is given in Table 14. Plume height is defined as the top of the plume after it has stopped rising and before significant dispersion has occurred.

Table 14. Summary of plume heights.

	Camera #1	**Camera #2**
June 5, 2012	146 ft ± 30 ft. (45 m ± 9 m)	207 ft ± 30 ft. (63 m ± 9 m)
June 6, 2012	256 ± 40 ft. (78 m ± 12 m)	276 ± 40 ft. (84 m ± 12 m)
June 7, 2012	138 ± 20 ft. (42 m ± 6 m)	malfunction

The difference between the measurements from the two cameras for each burn is consistent with the estimated uncertainty of about 15%, although the June 5 burn is at the limits of those uncertainties.

cc: San Le, Org 6233
Dan Clayton, Org 6223

Distribution:

3	US Department of Energy, NE-75 Office of Radioisotope Power Systems Attn: Ryan D. Bechtel, (2) Attn: Scott Harlow, (1) 19901 Germantown Road Germantown, MD 20874	
2	Tetra Tech, Inc. Attn: Steve Giannino (2) 20251 Century Boulevard, Suite 200 Germantown, MD 20874-7114	
3	Johns Hopkins University, 1E-255 Attn: Yale Chang (3) Applied Physics Laboratory 11100 Johns Hopkins Road Laurel, MD 20723	

1	MS0747	Charles W. Morrow, 6223
2	MS0747	Daniel J. Clayton, 6223
1	MS0747	Fred Gelbard, 6223
1	MS0748	Nathan E. Bixler, 6232
1	MS0744	San Le, 6233
1	MS0899	Technical Library, 9536 (electronic copy)

Sandia National Laboratories